

Sustainable Design Framework for Enhancing Shear Capacity in Beams Using Recycled Steel Fiber-Reinforced High-Strength Concrete

Qin, Xia; Huang, Xu; Li, Yang; Kaewunruen, Sakdirat

DOI:

[10.1016/j.conbuildmat.2023.134509](https://doi.org/10.1016/j.conbuildmat.2023.134509)

License:

Creative Commons: Attribution (CC BY)

Document Version

Publisher's PDF, also known as Version of record

Citation for published version (Harvard):

Qin, X, Huang, X, Li, Y & Kaewunruen, S 2024, 'Sustainable Design Framework for Enhancing Shear Capacity in Beams Using Recycled Steel Fiber-Reinforced High-Strength Concrete', *Construction and Building Materials*, vol. 411, 134509. <https://doi.org/10.1016/j.conbuildmat.2023.134509>

[Link to publication on Research at Birmingham portal](#)

General rights

Unless a licence is specified above, all rights (including copyright and moral rights) in this document are retained by the authors and/or the copyright holders. The express permission of the copyright holder must be obtained for any use of this material other than for purposes permitted by law.

- Users may freely distribute the URL that is used to identify this publication.
- Users may download and/or print one copy of the publication from the University of Birmingham research portal for the purpose of private study or non-commercial research.
- User may use extracts from the document in line with the concept of 'fair dealing' under the Copyright, Designs and Patents Act 1988 (?)
- Users may not further distribute the material nor use it for the purposes of commercial gain.

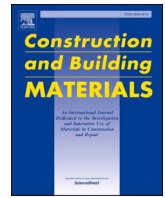
Where a licence is displayed above, please note the terms and conditions of the licence govern your use of this document.

When citing, please reference the published version.

Take down policy

While the University of Birmingham exercises care and attention in making items available there are rare occasions when an item has been uploaded in error or has been deemed to be commercially or otherwise sensitive.

If you believe that this is the case for this document, please contact UBIRA@lists.bham.ac.uk providing details and we will remove access to the work immediately and investigate.



Sustainable design framework for enhancing shear capacity in beams using recycled steel fiber-reinforced high-strength concrete

Xia Qin^a, Xu Huang^a, Yang Li^b, Sakdirat Kaewunruen^{a,*}

^a Department of Civil Engineering, School of Engineering, University of Birmingham, Edgbaston B15 2TT, UK

^b Key Laboratory of Roads and Railway Engineering Safety Control (Shijiazhuang Tiedao University), Ministry of Education, Shijiazhuang 050043, China

ARTICLE INFO

Keywords:

Shear improvement
Recycled steel fibre
Shear deficiency
Waste management
Sustainable design framework

ABSTRACT

According to a recent estimate, over 1.5 billion wasted tyres which containing over 40% of vulcanised rubber and 15% of steel fibre are discarded yearly, which posing a serious threat to circular economy implementation and transition to net zero. To minimise the greenhouse gas (GHG) emission and the environmental side effect caused by burning and burying these waste tyres, recycling and reusing these materials for sustainable structural designs has become the centre of attention. This paper focuses on applying recycled bead steel fibre to improve the shear capacity of fibre-reinforced concrete beams. Moreover, the existing national standard known as Eurocode 2 and TR63 can hardly illustrate the relationship between fibre and high-strength concrete. This study is the first to investigate shear behaviours of high-strength industrial and recycled steel fibre reinforced concrete beams with consideration of different shear span ratios. Therefore, twenty real-scale beams are constructed to examine the shear capacity of high-strength industrial and recycled steel-fibre reinforced concrete beams, which aims to compare the improvement of shear strength through experiments and identify different shear strength improvements of the two categories of steel fibre. Besides, comprehensive data of 164 beams from previous studies have been collected to benchmark with the experimental results for the formula design. This study proves the feasibility of replacing industrial steel with recycled steel fibre to improve the shear capacity of fibre-reinforced concrete beams. Moreover, there are six novel equations designed developed using Eurocode 2 and TR63 as a basis in this study. Based on the findings of the paper, the proposed formulas demonstrate remarkable accuracy, with an average value of 0.982 and standard deviation of 0.213, respectively. Following an exhaustive comparison of RSF and ISF reinforced concrete beams, with a focus on economic expenditure and GHG emissions, it can be concluded that RSF offers superior economic and environmental benefits, which reduce the emissions up to 25.39% and price up to 28.04% when replacing ISF 0.8% RSF, respectively.

1. Introduction

Circular economy implementation is at risk of failing due to the lack of pragmatic technical solutions to manage end-of-life assets and to reduce industry wastes. With the rapid expansion of automobile consumption worldwide, waste tires which is known to potentially endanger the environment, continues to exhibit a continuous upward trend. In an appropriately constructed tyre, roughly fifty percent is made up of natural rubber, butadiene rubber, and styrene-butadiene rubber. The remaining composition includes elements like carbon black, metals, textiles, zinc oxide, sulfur, and various additives [1]. With all these chemicals and materials in a bundle, wasted tyre disposal has become a significant concern for the ecology because of the non-biodegradable

nature of wasted rubber, making proper disposal of used tyres a critical environmental issue [2]. For example, the Europe Union member alone produces more than three million tons of used tyres, with 4 billion tyres currently in stock [3]. A variety of strategies have been suggested to handle these tyres post-usage, such as repurposing through recycling, re-treading, depositing in landfills, and using as fuel for energy production [4]. Among these proposals, re-treading tyres repeatedly are considered the most cost-effective way to delay the disposal problem. However, nevertheless, most tyres are still hoarded towards the end of their service lives. When tires are hoarded and left exposed to the elements, they can leach harmful chemicals such as heavy metals, polycyclic aromatic hydrocarbons (PAHs), and other toxic substances into the soil and underwater. These chemicals have potential risks to the

* Corresponding author.

E-mail address: s.kaewunruen@bham.ac.uk (S. Kaewunruen).

<https://doi.org/10.1016/j.conbuildmat.2023.134509>

Received 31 May 2023; Received in revised form 25 November 2023; Accepted 7 December 2023

Available online 12 December 2023

0950-0618/© 2023 The Author(s). Published by Elsevier Ltd. This is an open access article under the CC BY license (<http://creativecommons.org/licenses/by/4.0/>).

local ecosystem, damaging plant and animal life. In comparison, recycling tyres is potentially the most sustainable approach to dealing with tyre wastes because the process has high added commercial value with the components, such as rubber, high tensile strength steel wires, and textile of rayon and nylon. In fact, decades of research on using recycled tyre materials in concrete composition has concluded in many solutions widely used in actual practice. For example, after recycling and incorporating tyre materials into concrete, the rubber granular, as a significant side material, is widely used in various infrastructure applications [5,6]. Similarly, as the second side material after tyre recycling, scraped steel can also be reused in industrial constructions. In this context, some studies have suggested shredding the bead wires and using that type of steel fibre (RSF) to improve the concrete performance and explore the possibility of replacing traditional industrial steel fibre (ISF) with RSF."

Previous studies show that adding artificial short fibres to concrete contributes to enhancing the fundamental strength of plain concrete and avoiding brittle and low tensile capacity because it improves the effectiveness of stress transfer from fibre to paste matrix [7], helping to arrest the excessive development of cracks in the paste [8]. According to related experimental results, adding ISF in reinforced concrete beams is beneficial to improving the ductile behaviour and the shear capacity while delaying the development of cracks [9]. In the mix design, adding a small amount of ISF provides operative shear resistance that changes the failure mode from shear to flexure. For example, Lantsoght [10] suggests that the tension of shear resistance is caused by fibre' creation of cracks. The efficiency of bridging effect depends on the fibre properties, such as fibre-matrix interfacial bonds, fibre fracture, fibre content, and fibre aspect ratio. However, random fibre can hardly be described with traditional mechanism formulas. Therefore, several previous studies [11,12] have attempted to model complex and compelling fibre bridges effect with key parameters to predict the shear strength of fibre-reinforced concrete beams and describe the improvement with the randomly added steel fibre. For instance, Mansur, Ong and Paramasivam [13] have established a model based on the ACI Committee 544, which aims to use a simplified formula to describe the shear failure mechanism of ISF-reinforced concrete beams. After obtaining the test results of 89 steel-fibre reinforced concrete beams, Al-Ta'an and Al-Feel [14] have built an empirical formula with the regression analysis. Besides, The TR63 published and developed based on Eurocode 2 has proposed utilising experimental results from crack mouth opening displacement (CMOD) bending tests to estimate tensile properties of steel-fibre reinforced concrete beams with simplified assumptions. Review the TR 63 and Eurocode 2, with the simplified CMOD test results, the synergistic behaviours among fibre, concrete matrix and longitudinal rebars cannot be described well. Moreover, shear span ratio, high strength concrete and the dimension effect has not been considered in the formula development of shear capacity. In order to improve the current design code, future research should consider additional factors such as high strength concrete (HSC), fibre types, and durability. HSC is not only tend to described the strength of the concrete but also refers to its outstanding comprehensive performance. It is extensively utilized in the construction of high-rise buildings and large-span bridges. The application of HSC has widely used in taller buildings and bridges with longer spans. According to the case study provided by YB, Hossiney and HT [15], a structure with 50 levels utilizing columns with a diameter of 1.22 m and concrete with a normal strength of 27.6 MPa can decrease the column diameters by about 33% by opting for concrete with a high strength of 55.2 MPa.

The majority of research has centred around incorporating ISF into normal-strength concrete to analyse the shear characteristics of ISF reinforced concrete beams. Review the TR 63 and Eurocode 2, both standards are originally aimed to introduce the design of normal-strength concrete but fail to describe the increasing synergistic effects between the fibre and concrete of high-strength concrete. Furthermore, with the increase of shear span, the failure mode and shear capacity of

beams will be changes which have not been discussed in TR63. Meanwhile, no previous study has focused on the performance of RSF in improving the shear capacity of ISF in fibre-reinforced concrete. Apart from making up for the gaps in previous studies, the next phase of this study will verify the effect of shear span on the RSF and ISF in high-strength beams without stirrups and shear failure. Therefore, this study conducts 20 full-scale shear tests with different shear span ratios ranging from 1.5 to 4 to determine the capacity of shear resistance, the strain distribution of the longitudinal rebar, the crack development, the ductility, and the failure mode. Then, the experimental results of shear capacity will be compared with the values predicted by different design approaches and standards. In this way, several predicted formulas will be proposed based on the experimental results. Furthermore, the TR63 and Eurocode 2 are also adopted to determine the shear behaviour of the RSF and ISF-reinforced concrete beams, in which 164 collected beam results which are collected from published literatures (Details shown in Appendix A-2), will be used to validate against experimental tests and the analysis. Moreover, this paper delves into the pivotal role of RSF within the context of the circular economy. The replacement of ISF with RSF not only reduce the need for mined iron ore, but also curtails environmental impacts. Using recycling materials for substitution significantly cuts down on the quantity of waste to be consigned to landfills.

2. Research significance

Shear is a type of force that acts perpendicular to the longitudinal axis of a structural component, such as a beam or a column. When a structural component is subjected to shear forces that exceed its capacity to resist them, it can suffer a sudden and catastrophic failure without any warning, leaving limited time for evacuation or other safety measures. The shear failure can result in property damage, injury, or loss of life, which is the most dangerous type of failure in the structure. In order to address this deficiency, the addition of steel fibres into concrete has become a widely utilized technique in component structures.

A critical review reveals that the application of RSF in concrete construction has a huge impact on sustainable development and cost reduction. Based on previous studies examining the mechanical properties of RSF reinforced concrete, it has been observed that the incorporation of RSF significantly enhances the tensile strength which shown the similar improvement efficiency of ISF [16]. Since the use of ISF increases the shear resistance of concrete beams has been identified, use of RSF to replace the function of ISF might be considered as one of the ways to reduce environmental impact and cost of structural components. In recent years, the concept of the circular economy has catch significant attention by society. Substituting ISF with RSF can play a crucial role in promoting this circular economic model [17]. Regarding environmental impacts, employing RSF reduces the need for mined iron ore, substantially decreases landfill waste, and enhances sustainability within the construction sector which plays an important role in reducing the global carbon emissions [18]. Economically, RSF is generally less costly than ISF, which can lower construction expenses[19]. From a societal perspective, using RSF can stimulate local economies while reinforcing the principles of the circular economy.

Although substantial research reports on the mechanical properties of RSF concrete as a substituent material to ISF in concrete are available, research work on structure design, particularly focusing on high-strength reinforced concrete beams, remains insufficient. Beams, being one of the most commonly used and critical structural elements, hold a significant place in structural systems. Studies that experimentally examine the shear performance, cost, and environmental impact of high-strength fibre-reinforced concrete beams using RSF are still lacking. Considering this critical gap in the current research landscape, this study was carried out to identify:

- The shear behaviours of using RSF in varying shear span ratios of high strength fibre reinforced concrete beams.
- Proposed formulas to evaluate the RSF and ISF in shear improvement of high strength fibre reinforced concrete beams.
- The contribution of using RSF replacing the ISF from the view of economic and environmental aspects.

In this study, 20 real-scale ISF and RSF reinforced concrete beams have been casted for experimental investigations, conducted to determine the effects of different types (RSF and ISF) on improving the shear resistance of concrete beams, with consideration of the impact of high strength concrete and different shear span ratio. Moreover, there are six novel empirical formulas proposed in this study by using the experimental results and collected datasets from published literature. Interesting findings in this study are investigating the experimental work with consider the effect of shear span ratio and high strength concrete, as well as proposing six novel formula design based on TR63 and Eurocode 2. Moreover, the contribution of RSF in the sustainable development was evaluated by the cost budget and green house emission analysis, which aims to give the following researchers a comprehensive identification about the sustainable and structural contribution with the using of the RSF.

3. Experimental programmes

3.1. Recycled steel fibre

Similar to the study of [20–25], this study uses a type of recycled steel fibre recovered from bead wires in tyres. To improve the performance of the RSF when shredding the beading wire, the RSF is bent with the hook end. As shown in Table 1, 50 fibre are selected randomly to check the dimension with a mean diameter of 1.62 mm, a length of 50.1 mm, and a tensile strength between 2400 and 2800 MPa [26]. Meanwhile, the ISF used in this study is supplied by SIKa. However, the hooked-end steel fibre has a diameter of 1 mm and 50 mm in length and an ultimate tensile strength of 1150 MPa. Fig. 1 serves as a comprehensive summary and review of the entire recycling process, which aims to illustrates the contribution of RSF to the circular economy, particularly emphasizing the distinct characteristics of the two types of fibres and underscoring the value of recycling tires. Based on the information provided in Fig. 1, it highlight the process of end-of-life tire from waste to valuable construction material. Moreover, according to the comparison between the appearance of RSF and ISF in Fig. 1, the surface of RSF is covered by black rubber powder produced when the tyre rotates at high speed in the steel wires recovery process, which may affect the fibre-cement interfacial bonding force.

3.2. Material properties

The composite of high-strength concrete (HSC) demonstrates exceptional mechanical robustness, notable longevity, limited permeability, and dense composition. In addition, it fulfils specific uniformity and performance standards, thereby outperforming traditional normal strength concrete. [27]. According to the guidelines set by the ACI committee, HSC as having a specified compressive strength of 8000 psi

(55 MPa) or greater[28]. Specifically, HSC sees extensive usage in long-span bridges and high-rise building due to its ability to withstand higher dead and live loads with fewer supporting piers, thereby extending the lifespan of these structures. [29]. Furthermore, as HSC facilitates the construction of larger columns, resulting in increased floor space and wider column spacing without impacting the lower floors negatively, it holds significant potential for use in tall buildings. [30]. However, previous studies have covered the behaviour of beams, such as the shear resistance and ductility, when embedded in the HSC, which is based on the mid-span deflection, failure mode, and crack growth. Since the shear failure of concrete members is affected by the increasing compressive strength, the failure caused by the high-strength concrete beam shear shows more brittle and explosive than normal-strength fibre-reinforced concrete beams [31]. In addition, solid wasted materials, such as used glass and recycled aggregate, can potentially be applied in HSC to overcome the lack of strength of the waste itself. In this way, HSC incorporated with solid wastes can enhance strength and sustainable prospects. Nevertheless, after a comprehensive review, very limited studies have considered the RSF embedded in the HSC, making the shear failure mechanism of RSF-reinforced concrete beams uninvestigated. Therefore, this study will focus on the shear span ratio, RSF and high-strength concrete to investigate the shear performance of high strength concrete beams with different shear span when RSF and ISF are added, respectively.

This study adopts the Ordinary Portland Cement 52.5 N, which meets the British Standard of High-strength Cement (BS EN 197–1-CEM I [32]). Meanwhile, natural river sand has been applied as a fine aggregate with a specific gravity of 2.5 and a bulk density of 1700 kg/m³. In addition, the crushed granite is 10 mm, which is the nominal size as coarse aggregate with a specific gravity of 2.5 and bulk density of 1650 kg/m³. According to Table 2, which describes the five groups of mixture proportions of ISF and RSF-reinforced concrete, the fibre volume fraction is of 0.4% and 0.8%, with a water-to-binder ratio of 0.45, respectively. Selection of volume fractions exceeding 1% should be avoid, because it will affect the workability of the concrete. Specifically, higher volume fractions lead to significant balling effects of fibres in concrete, which will not only reduce the slump of the mixture, but also increase the potential risk of void hole. This phenomenon can lead to the formation of undesirable properties in the concrete, such as honeycombs and voids, which is particularly prevalent during the casting process. Furthermore, the experimental setup involves the use of steel cages, which requires the concrete mix to maintain a certain level of workability to prevent the occurrence of such defects. Mixtures with low slump may result in the balling effect and the concentrated fibre distribution. Therefore, to ensure the general applicability and relevance of our experimental results, we strategically chose to use volume fractions of 0.4% and 0.8%. This decision is based on standard industry practice and seeks to balance the benefits of RSF and ISF in improving the shear strength of high-strength concrete beams while remaining practical and realistic in concrete construction. On the other hand, the plain concrete in the contrast group without the addition of fibre has also been developed to reveal how the fibre enhance tensile strength.

3.3. Test specimen and setup

The compressive strength of ISF and RSF-reinforced concrete has been tested with the British Standard of BS EN 12390–3, with a loading rate of 0.5 MPa/s. Meanwhile, according to the illustration of the cross-section and reinforcement design of ISF and RSF beams for the shear strength tests in Figs. 2, 3 and 4, the beam specimens have suffered a failure due to the three-point loading with a 500 kN capacity of deflection control with a hydraulic machine. In addition, vertical deflections have been measured with a laser displacement monitor (LDM) under the loading positions.

The experimental programme consists of 20 ISF and RSF-reinforced beams with a length of 1500 mm. The four different spans measure

Table 1
Comparison between the RSF and ISF.

	RSF	ISF
Tensile Strength	2400 ~ 2800 MPa	1150 MPa
Raw Material	Scarp bead wire	Steel plate
Diameter	1.62 mm	1 mm
Length	50.1 mm	50 mm
Aspect Ratio	30.92	50
Surface	Covered by Rubber Dust	Clean

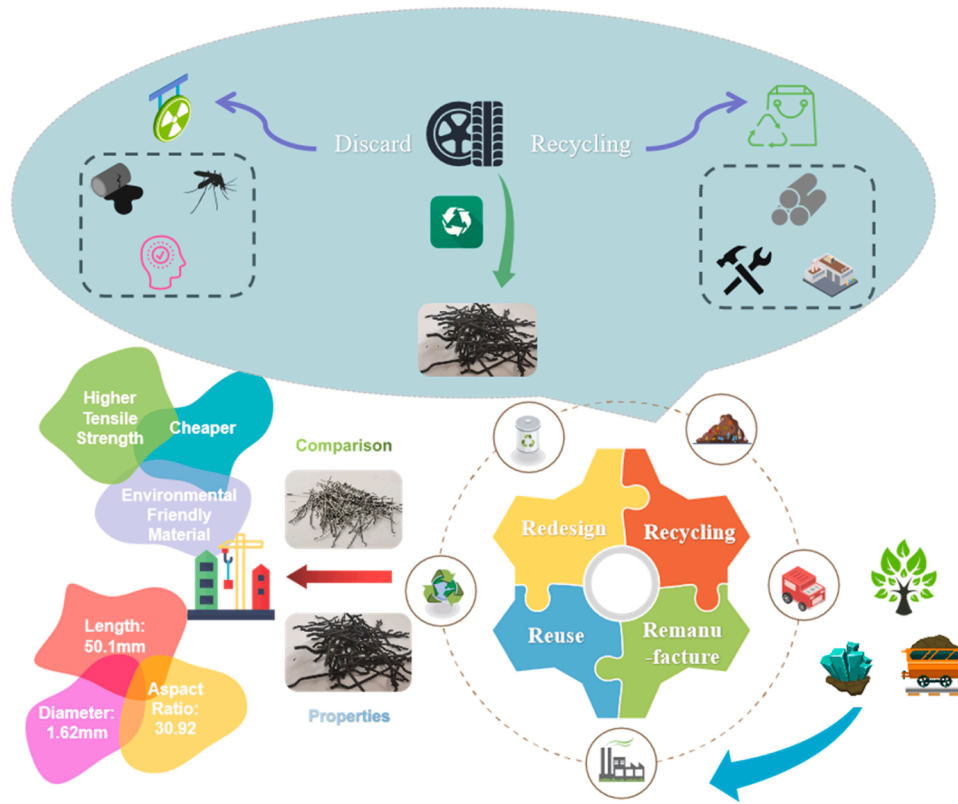


Fig. 1. Application of RSF in circular economy.

Table 2
Concrete Mix.

Group	Cement (kg/m ³)	Water (kg/m ³)	Sand (kg/ m ³)	Gravel (kg/m ³)	Fibre (kg/m ³)
Plain Concrete	317.3	171.34	983.63	713.925	0
0.4 ISF	317.3	171.34	983.63	713.925	24(0.4%)
0.8 ISF	317.3	171.34	983.63	713.925	48(0.8%)
0.4 RSF	317.3	171.34	983.63	713.925	24(0.4%)
0.8 RSF	317.3	171.34	983.63	713.925	48(0.8%)

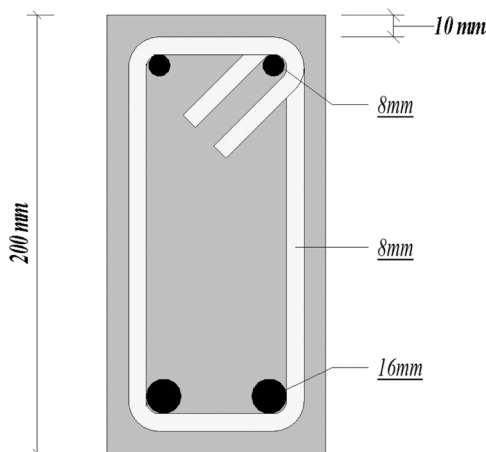


Fig. 2. : Details of cross-section.

260 mm, 432 mm, 608 mm, and 698 mm, with a standard rectangular cross-section standing 200 mm tall and 100 mm wide. In the shear span area, no stirrups are placed to assist the shear failure, but the rest of the specimen has been reinforced with Ø10 stirrups spaced at 90 mm for the shear spans of 1.5, 2.5 and 3.5 to avoid the shear failures of the beams even after applying the retrofit solutions. For the beams with a shear span of 4, extra stirrups are used to avoid shear failure of the non-failure areas, with the details shown in Fig. 3. Additionally, the bottom longitudinal reinforcement of the beams comprises two Ø16 mm bars, while the top is reinforced with two bars of a nominal Ø8 mm diameter. Both the top and bottom reinforcements are arranged in a single layer. Moreover, the concrete cover of the bottom reinforcement is 10 mm, with the beam specimen details summarised in Table 3. The purpose of the experiment is to characterize the shear performance of ISF and RSF reinforced concrete beams without stirrups.

Each experimental specimen is labelled with three-subscript symbols with a dash. The first symbol denotes the concrete mix, with M0 as plain concrete, M1 as 0.4% fibre-reinforced concrete, and M2 as 0.8% fibre-reinforced concrete. Then, the second symbol indicates the fibre type, with R referring to RSF and I representing ISF. Finally, the last symbol stands for the shear span ratio, with $S = 1.5, 2.5, 3.5$ and 4. As described in Table 2, although the beams have similar geometric properties, reinforcement, and target compressive strength, they can be differentiated by the fibre content, type, and shear span ratio. For example, four control beam specimens have been cast with fibre content equal to zero but with different shear span ratio. On the other hand, the fibre content in the seventeen remaining specimens is 0.4% and 0.8%.

4. Experimental results and discussion

4.1. Compressive strength test

According to the results of the compressive strength of ISF and RSF concrete displayed in Fig. 5, the specimens enforced with ISF and RSF

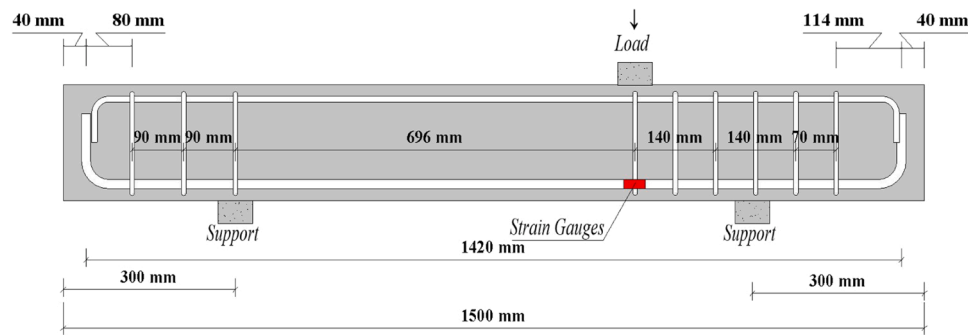
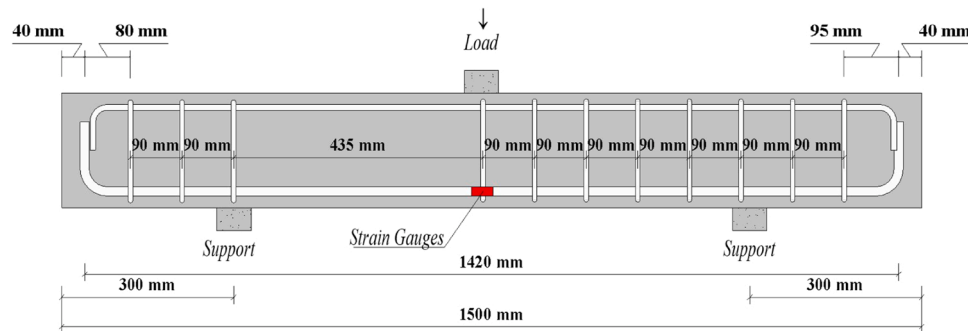
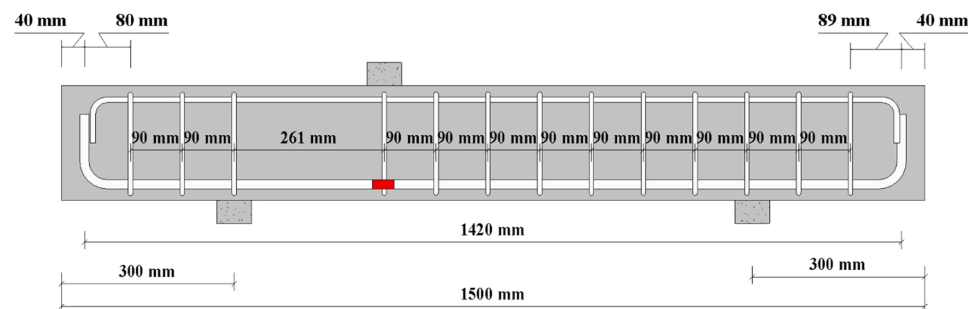


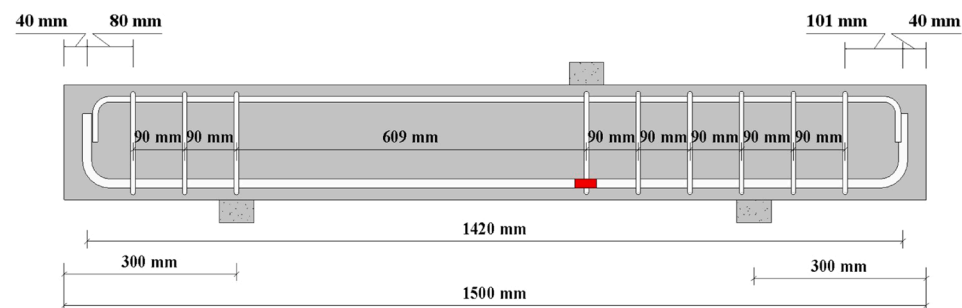
Fig. 3. : Details of beam dimension with shear span ratio of 4 (unit is mm).



(a) Shear span ratio of 2.5



(b) Shear span ratio of 1.5



(c) Shear span ratio of 3.5

Fig. 4. : Details of beam dimension of shear span ratio from 1.5 to 3.5 (unit is mm).

have exhibited a gradual compressive strength that increases with the addition of fibre content. However, limited compressive strength improvement is presented, indicating that adding steel fibre can slightly affect compressive improvement. Besides, the improvement can be explained by the higher stiffness of fibre than matrix. The ISF ratio

variation from 0% to 0.4% and 0.8% % has increased the concrete compressive strength by around 4.2% and 9.4%, respectively. Furthermore, the compressive strength of the RSF concrete specimens is 0.4% and 0.8% of fibre content compared to plain concrete, which has increased by 2.4% and 6.6% for mixing with RSF, respectively.

Table 3
Beams information.

Beam	Shear Span Ratio	Shear Span (mm)	Effective Depth (mm)	Longitudinal Ratio (%)	Fibre Content (%)
M0-1.5	1.5	260	174	2	0
M0-2.5	2.5	432	174	2	0
M0-3.5	3.5	608	174	2	0
M0-4	4	696	174	2	0
M1- ISF-1.5	1.5	260	174	2	0.4
M1- ISF-2.5	2.5	432	174	2	0.4
M1- ISF-3.5	3.5	608	174	2	0.4
M1- ISF-4	4	696	174	2	0.4
M2- ISF-1.5	1.5	260	174	2	0.8
M2- ISF-2.5	2.5	432	174	2	0.8
M2- ISF-3.5	3.5	608	174	2	0.8
M2- ISF-4	4	696	174	2	0.8
M1- RSF-1.5	1.5	260	174	2	0.4
M1- RSF-2.5	2.5	432	174	2	0.4
M1- RSF-3.5	3.5	608	174	2	0.4
M1- RSF-4	4	696	174	2	0.4
M2- RSF-1.5	1.5	260	174	2	0.8
M2- RSF-2.5	2.5	432	174	2	0.8
M2- RSF-3.5	3.5	608	174	2	0.8
M2- RSF-4	4	696	174	2	0.8

According to Fig. 5, adding RSF to replace ISF has lowered the compressive capacity of the mixture, but the gaps are limited. The addition of RSF and ISF does not significantly improve the compressive strength. This finding aligns with the results obtained by Johnston and Skarendahl [33], who noted that fibres have a minimal improvement effect on the compressive strength. However, this improvement is mainly depends on the types and quantities of fibres.

The conclusion can be drawn that the incorporation of both ISF and RSF enhances the compressive strength of concrete. This can be attributed to the fact that the inclusion of fibres, especially ISF, enhances the bonding among the concrete components and aids in increasing the bridge effect of stress concentration and both micro and macro cracks. Furthermore, by increasing the ratio of both types of steel fibre, the slope showing the compressive strength of the ISF concrete curves with the addition of fibre concrete higher than the RSF concrete curve. However, the curves of ISF and RSF concrete are close.

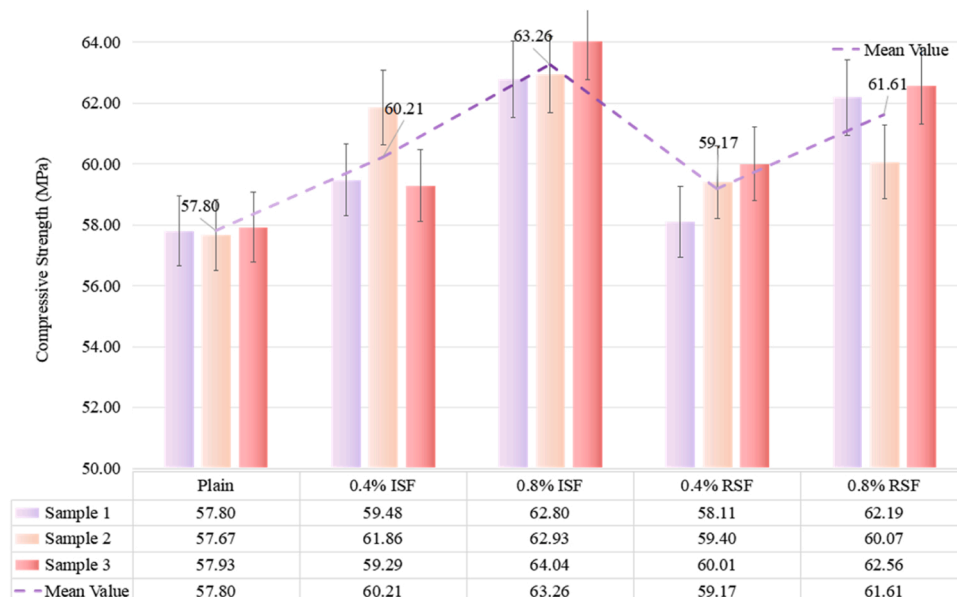
4.2. Shear strength test

This section highlights the effect of ISF/RSF on the shear improvement and cracking of 20 reinforced concrete beams made without stirrups. The tested beams are developed with different types of steel fibre, with different fibre volume fractions of 0%, 0.4%, and 0.8%. According to the experimental results given in Table 4, P_u and Δu are the ultimate shear force and corresponding deflection at mid-span, respectively; V_u and ϵ_u stand for the ultimate shear capacity and corresponding stains on the surface of longitudinal rebars at mid-span, respectively, and % u and % P refer to the ultimate shear capacity and corresponding displacement improvement ratio with respect to plain concrete beams, respectively.

The experimental findings have allowed for a selective consideration and comparison of aspects such as shear capacity, failure modes, crack patterns, deflection behaviour, and shear versus steel strain response across all tested specimens. In particularly, owing to the failure modes and ultimate shear forces of different beams with RSF caused by different fibre volume fractions, different shear span ratios are highlighted.

4.3. Load versus deflection curves

The curves plotting load versus mid-span deflection for the beam specimens are divided into numerous groups, based on the relevant

**Fig. 5.** : Compressive Strength.

variables under consideration as presented in Figs. 6, 7, 8, and 9. In our study, the stiffness in the elastic region was determined using the load-displacement curves obtained from the experimental results. The stiffness was calculated as the slope of this linear segment of load displacement curve.

As shown in Fig. 6, beams with ISF and RSF of shear span ratio of 1.5 have significantly improved the stiffness and ultimate load capacity compared to M0–1.5, their counterpart beam. As per the experimental findings, the shear resistance of composite beams can be significantly enhanced by the addition of ISF and RSF. Meanwhile, although RSF-reinforced concrete beams contribute to the increasing shear capacity, their shear resistance improvement is less than ISF-reinforced concrete beams. Moreover, adding 0.8% of RSF, a higher volume of fibre, can increase the beams' stiffness, allowing them to sustain a higher ultimate load with larger corresponding deflections, which indicates a less brittle performance and a noticeable improvement in the energy absorption of the tested beams. The beams' ISF and RSF content accounts for 0.8% of the total volume, showing 49.94% and 36.26% increases in the load capacity, respectively. Notably, adding any type of fibre can enhance the stiffness and shear strength of fibre-reinforced beams compared to those without fibre. Besides, the enhancement rate of ISF and RSF are similar, mainly due to the limited fibre reinforcement area. According to Fig. 4, the fibre enhancement area of beams with a shear span ratio of 1.5 is less than other beams, meaning that the fibre amount in the enhancement area remains less than other beams with a higher shear span ratio. In these cases, the shear improvement by different types of fibre will be insignificant.

Group II has been obtained to study the shear capacity of fibre-reinforced concrete beams with a span ratio of 2.5, with M0–2.5, the control group specimen, exhibiting shear failure. When the load P reaches 40 kN, the shear cracks are initiated at the mid-span. Meanwhile, the majority of the cracks are located on both sides of the line between the loading point and the support, which are parallel to this line. Besides, the stiffness of the beam gradually degrades with the increasing cracks. After M1-ISF-2.5's peak strength (P_u) of 77.67 kN at the δ value of 5.59 mm, the load-bearing capacity is significantly decreased. Ultimately, the load-bearing capacity is increased to 220.6% of the peak strength with 0.8% of the ISF content and 171.3% of the peak strength with 0.8% of the RSF content. Furthermore, regarding the control specimen, the shear capacity of M1-ISF-2.5 and M1-RSF-2.5 has been increased by about 120.43% and 71.00%, respectively.

In relation to the beams in Group III and IV, the shear cracking load is particularly prominent in beams with a shear span ratio of 4, as the load-

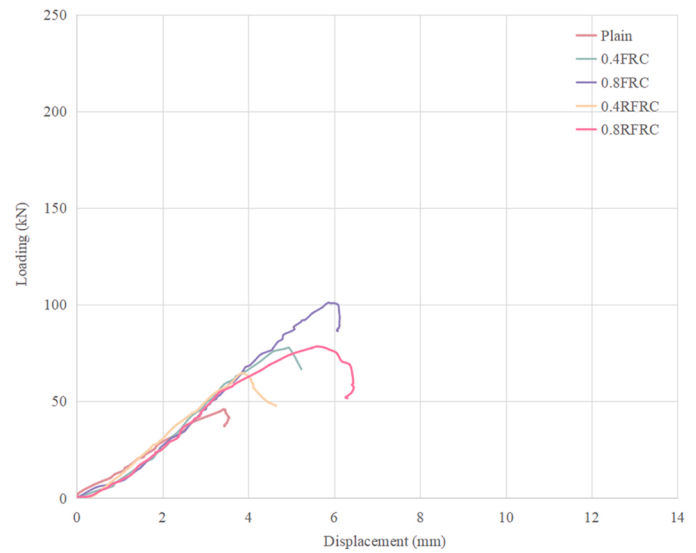


Fig. 7. Load Displacement Curve with a shear span of 2.5 (Group II).

deflection curve markedly diverges from the initial stiffness curve at the shear cracking point. Meanwhile, the stiffness of high-strength fibre-reinforced beams exhibits a gradual alteration with the addition of fibre, suggesting that the steel fibre provides a comparatively higher bridge effect as the shear span-to-effective depth ratio escalates. Therefore, compared to the control specimen, the shear capacity improvements are 30.39%, 49.16%, 29.45%, and 43.85% for beams M1-ISF-3.5, M2-ISF-3.5, M1-RSF-3.5, and M2-RSF-3.5, respectively. Moreover, the displacements at maximum shear load are significantly improved for the Group IV beams by adding steel fibre because it is the largest shear span among all groups. Compared to beam M0–4, the increases in deflection are 1.89%, 13.98%, 21.79% and 21.03% for beams M1-ISF-4, M2-ISF-4, M1-RSF-4 and M2-RSF-4, respectively. In addition, the shear strength improvements are 55.71%, 96.54%, 25.85% and 67.05%, respectively.

The assessment of the complete load-deflection response can be split into several phases: shear cracking, steady growth of shear load, and descending stages. During the stage of curve formation, the bridging impacts offered by the fibre aren't substantial, with all beams displaying nearly linear behaviour. Subsequently, as the load nears its peak value, the fibre ratio escalates along with the load rate and corresponding deflection. Moreover, with the increase in the shear span/depth ratio (a/d ratio), the differences in the ultimate load and deflection between the control specimens and those reinforced with RSF and ISF become more distinct in each figure. Interestingly, RSF beams show a load-deflection response at the midpoint nearly identical to that of ISF-reinforced beams with equivalent fibre concrete, implying that RSF-reinforced beams exhibit similar macro mechanical behaviours to ISF-reinforced beams with the same fibre content. Even though all beams exhibit brittle shear failure, as illustrated in Fig. 9, the downward phase of the load-deflection curve isn't immediately steep for beams reinforced with ISF and RSF. Intriguingly, when the shear span ratio attains 4 for the fibre-reinforced beams, the load increases along with a larger deflection as it nears the beams' maximum capacity, demonstrating that a higher shear span ratio can provide early warning due to the more substantial deformation occurred, which represents greater energy dissipation as the load nears its peak value.

The enhancement in shear resistance has been particularly notable in the lower shear span/depth ratio range from 1.5 to 2.5. Even though beams fortified with steel fibre have the same nominal theoretical shear contribution, those reinforced with ISF can attain marginally higher shear resistance compared to RSF-reinforced beams. As expected, the shear resistance strengthened by steel fibre increases nearly linearly with the increment of fibre content. However, as the shear span/depth

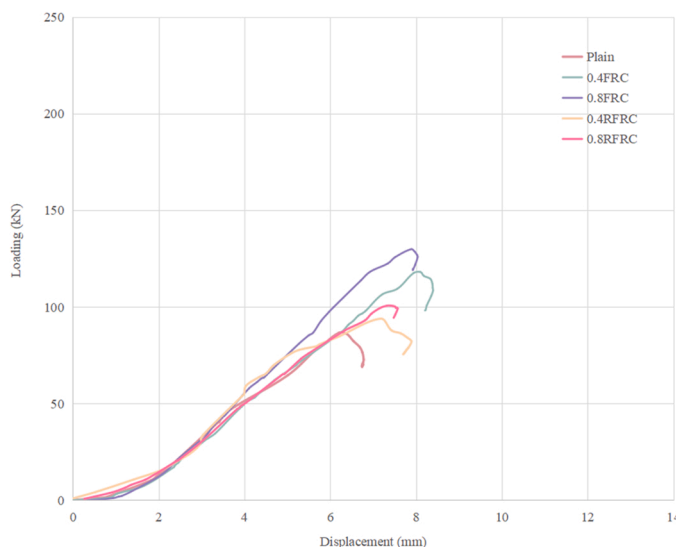


Fig. 6. : Load Displacement Curve with a shear span of 1.5 (Group I beams).

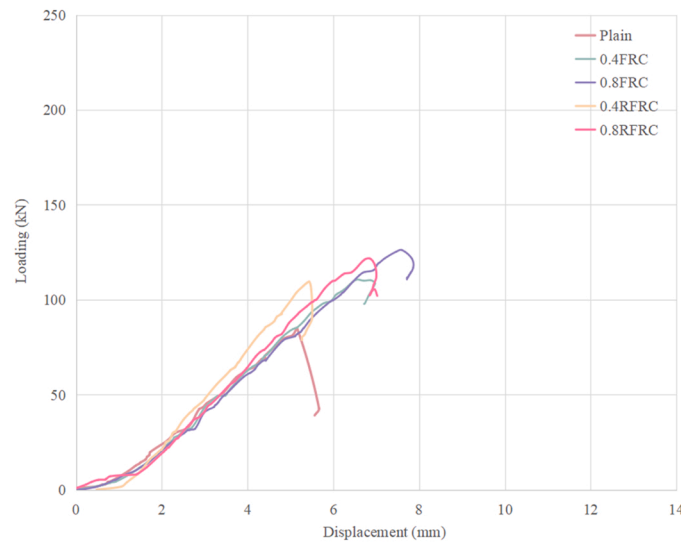


Fig. 8. : Load Displacement Curve with a shear span of 3.5 (Group III).

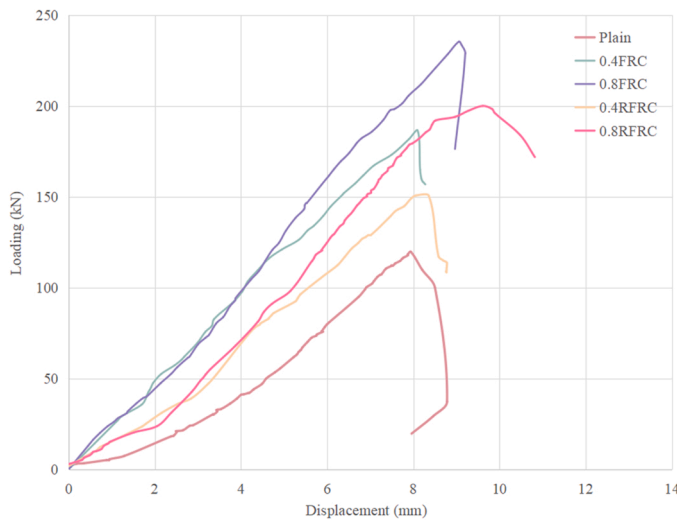


Fig. 9. : Load Displacement Curve with a shear span of 4 (Group IV).

ratio escalates from 2.5 to 4, the increase in shear resistance is not substantial. To sum up, both the shear span ratio and fibre content significantly influence shear resistance. Concurrently, the efficacy of RSF and ISF in enhancing shear resistance is analogous when maintaining same fibre content.

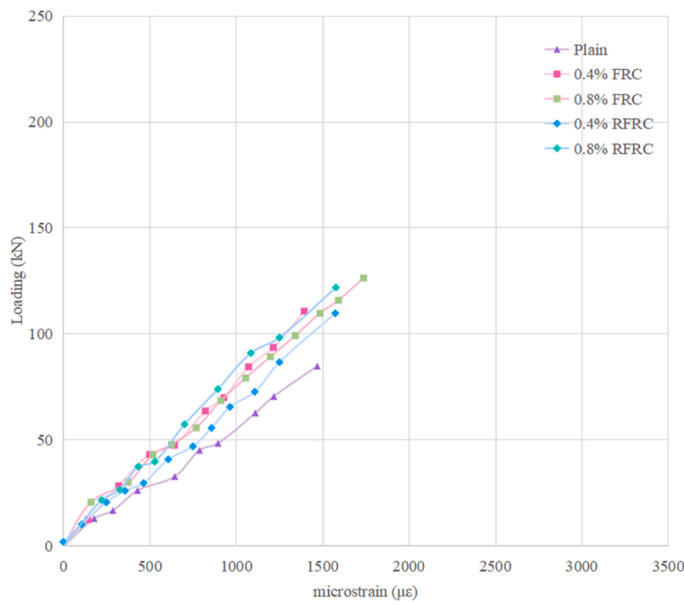
4.4. The strain of longitudinal reinforcement

The strains developed in the steel bars, recorded by the electrical resistance strain gauges strategically positioned at the midpoint of the load application area on each longitudinal steel bar (Details as shown in Figs. 3 to 5), are illustrated in Fig. 10 and Table 4. The maximum value of recorded strain from the strain gauges of the Group I beams has been $1823.6 \mu\epsilon$ with a shear span ratio of 1.5. Meanwhile, adding fibre is beneficial to improving the effective of shear resistance of longitudinal rebar, which mainly due to the synergistic behaviours between fibre and steel rebar. With the addition of fibre, of diagonal shear crack will be steeper which increasing the work area of longitudinal rebar. Review the performance of RSF, which contributes to a less cooperative relationship with steel rebars, even with substantial shear capacity improvement, mainly due to the weak hooked end. Besides, since the RSF is soft and

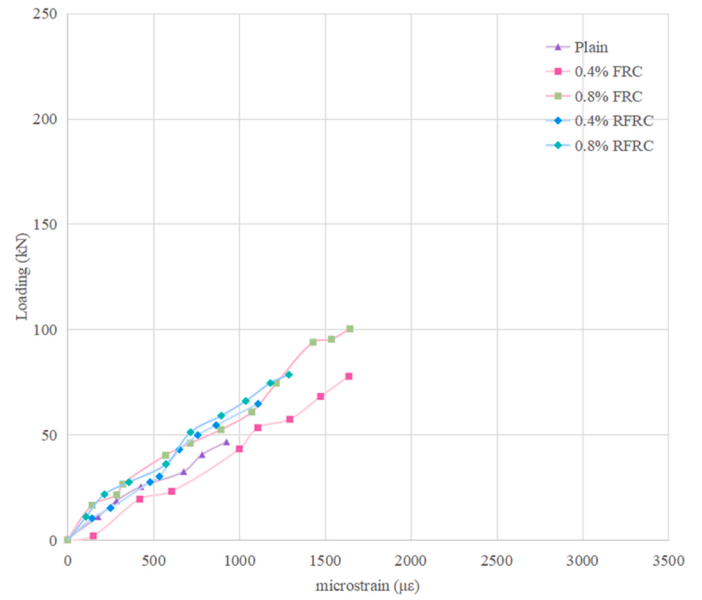
weak after being recovered from waste tyres with severe tire and wear, the fatigue effect can increase the potential risks of failure of the joint after being manufactured with the hooked end. According to the description of the relationships between the applied loads and strains in longitudinal rebar bars in Fig. 10, the strains in the longitudinal bar have increased significantly with the increased loading. Similar to Group I, it is no surprise that the maximum strains in longitudinal bars of RSF beams do not exceed the ultimate strains of ISF bars in reinforced concrete beams, with the maximum strain of $1645.47 \mu\epsilon$, as recorded for M2-ISF-2.5. Moreover, as demonstrated in the Group III beams with a shear span ratio of 3.5 and the Group IV beams with a shear span ratio of 4, as shown in Figs. 3 and 4, the maximum strains in longitudinal bars increase sharply for the shadow beams (shear span ratio ≥ 2.5), which can be directly seen with the increase of shear span ratio.

As per the crack pattern of the tested beams at failure presented in Appendix A-1, the Group I beam with a shear span ratio of 1.5 exhibits a deep-beam failure mode. Concurrently, a sequence of diagonal cracks is visible in the shear span, disrupting the horizontal shear transfer from the longitudinal reinforcement to the compression zone. Furthermore, the classic arch action significantly contributes to the shear resistance mechanism, with a few inclined cracks and concrete splitting involved in the failure process. In the initial loading stage, the applied load is borne by an uncracked concrete section until the emergence of the first crack. As the load escalates, cracks surface in the shear span regions and extend diagonally towards the loading points at angles ranging from 32 to 40 until sudden failure originates from a single major shear crack. Conversely, the beams with 0.4% and 0.8% ISF (B7 and B8) fail due to the formation of a single major diagonal crack, exhibiting a shear failure mode akin to the beams reinforced with RSF. The failure patterns also reveal that the inclusion of steel fibre diminishes the space between the cracks. Additionally, employing 0.8% ISF or RSF effectively reduces the crack openings due to the stitching action of the fibre, inducing tensile stress across the cracks, leading to an increase in delayed local crack. Post the diagonal crack, the extension of existing cracks is primarily seen with the increase in load. Further, the cracks interconnect with each other, gradually shaping a main failure crack.

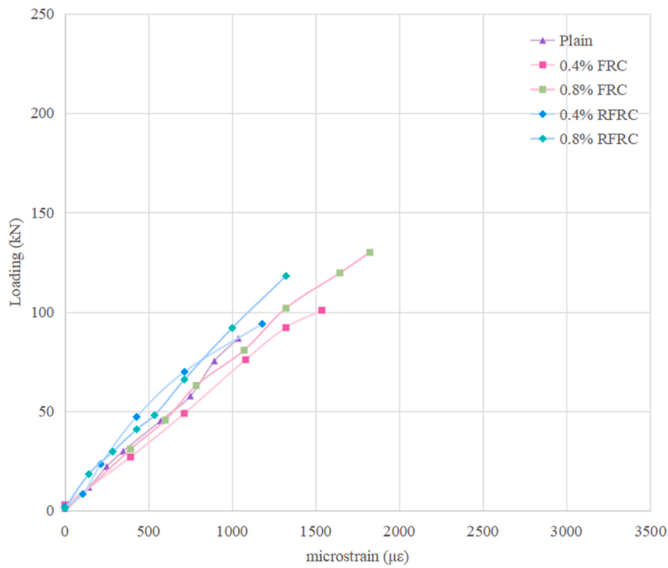
The failure mode that has appeared in all Group II beams with a shear span ratio of 2.5 is shear compression, as depicted in Appendix A-1. Although the brittle shear failure mode is typical among the Group II beams, the beams reinforced by steel fibre still show a much gentler failure mode than the control beams during the test. As the shear reinforcement ratio increases, a higher shear load can be obtained when specimens are near the ultimate state because the tension force is



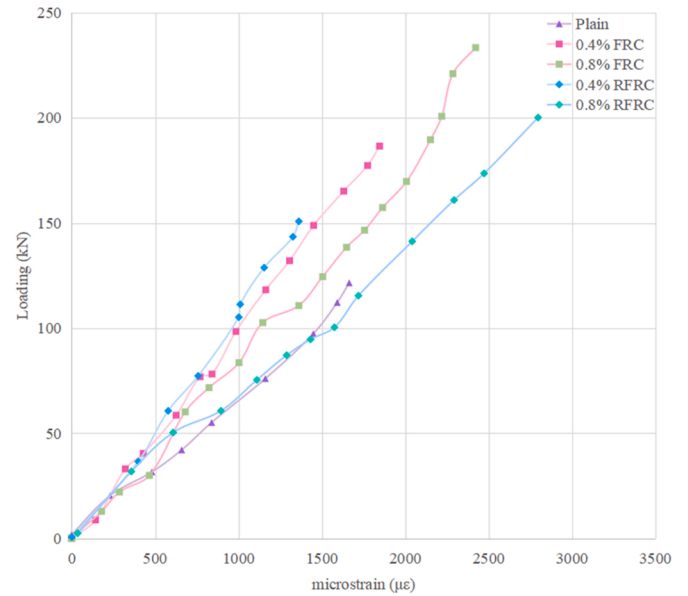
(a) Shear Span ratio of 1.5 (Group I)



(b) Shear Span ratio of 2.5 (Group II)



(c) Shear Span ratio of 3.5 (Group III)



(c) Shear Span ratio of 4 (Group IV)

Fig. 10. Loading strain curve.

resisted by steel fibre at the crack interface of the fibre-reinforced concrete beams, which increases the cracking and shear resistance. In specimens with a shear span ratio of 2.5, macro cracks are initiated following the line between the loading point and support when the loading reaches the ultimate state. However, most cracks forms to connect and develop around the main diagonal crack. Compared to the Group I beams with a shear span to depth ratio of 1.5, the results demonstrate a slight increase in the number of cracks and a decrease in crack width when the crack angle significantly drops with the addition of ISF. Furthermore, similar trends can be observed in beams with RSF-reinforced concrete with specific crack angles.

As depicted in [Appendix A-1](#), all the Group III and IV beams have failed in a flexural-shear mode. The first inclined shear cracks typically surface in the middle section of the concrete web. Subsequently, as the shear load amplifies, the width of the shear crack rapidly expands.

Secondary shear cracks also develop in the progression of prominent shear cracks. Similar to the Group II beams, the M0-4 specimens exhibit the mildest failure mode in comparison to the M0-2.5 and M0-3.5 beams. These test outcomes are not replicated in the Group I beams as their failure is primarily triggered by the crushing of the concrete compression strut. Compared to Group II, the substantial rise in shear resistance with the increase in the shear span-to-depth ratio is primarily due to the augmented vertical shear instigated by the steeper angle of the diagonal shear crack.

Review the failure mode of the 20 beams, the plain concrete beams single diagonal crack that propagates rapidly through the beam until it eventually fails. Upon reviewing the failure modes of the twenty beams, it becomes apparent that the shear resistance provided by the ISF or RSF increases as the shear-span ratio gradually increases. Compared to concrete beams without fibres, fibre reinforced concrete beams exhibit a

Table 4

The tested results of fibre reinforced concrete beam with ISF and RSF.

Beam	P _u	Δu	ε _u	%u	%P	V _{cr}
M0-1.5	86.65	6.21	1037.5	-	-	3.54
M0-2.5	45.86	3.41	926.47	-	-	1.36
M0-3.5	84.58	5.16	1469.76	-	-	1.57
M0-4	119.78	7.94	1663.98	-	-	1.56
M1- ISF-1.5	100.8	7.41	1537.2	16.33%	19.32%	4.11
M1-ISF-2.5	77.67	5.59	1639.09	69.36%	63.93%	2.31
M1- ISF-3.5	110.28	6.86	1394.77	30.39%	32.95%	2.05
M1- ISF-4	186.51	8.09	1845.83	55.71%	1.89%	2.43
M2- ISF-1.5	129.92	7.889	1823.6	49.94%	27.04%	5.30
M2- ISF-2.5	101.09	5.87	1645.47	120.43%	72.14%	3.00
M2- ISF-3.5	126.16	7.60	1737.7	49.16%	47.29%	2.34
M2- ISF-4	235.42	9.05	7.59	96.54%	13.98%	3.07
M1- RSF-1.5	93.94	7.17	1180.3	8.41%	15.46%	3.83
M1-RSF-2.5	64.60	3.84	1110.22	40.86%	12.61%	1.92
M1- RSF-3.5	109.49	5.44	1574.42	29.45%	5.43%	2.03
M1- RSF-4	150.74	9.67	1362.46	25.85%	21.79%	1.96
M2- RSF-1.5	118.07	8.10	1322.8	36.26%	30.43%	4.82
M2- RSF-2.5	78.42	5.59	1289.98	71.00%	63.93%	2.33
M2- RSF-3.5	121.67	6.85	1577.79	43.85%	32.75%	2.26
M2- RSF-4	200.09	9.61	2796.47	67.05%	21.03%	2.61

milder mode of failure. For beams with a large shear-span ratio, the addition of fibres changes the failure mode from direct shear failure to a combination of shear and flexural failure. The addition of fibres has a significant effect on impeding the rapid progress of cracks. In the examination of beams with a larger shear-span ratio, it was investigated that concrete beams reinforced with fibres display partial small cracks prior to the onset of major diagonal cracks. In addition, during the phase of swift crack development, the fibres effectively hinder the rapid spread of cracks, which makes it possible for people to evacuate and relocate their possessions before structural failure arises. Adding RSF reinforcement in the beams will result in a significant improvement in the cracking patterns. Initially, the interaction between steel fibre and the longitudinal reinforcements exhibits uniformly distributed fine cracks while eliminating the early strain localisation. Meanwhile, the higher fibre content in the beams has improved the serviceability limits with a noticeable reduction in the crack width. Moreover, the RSF can reach the same performance as ISF while controlling crack development, indicating that the bridging effect provided by RSF delays the brittle shear failure, thereby enhancing the ductility of the strengthened specimens.

5. The shear capacity prediction based on TR63

5.1. Analysis of existing formulas

In the fibre-reinforced concrete beam structure, the added fibre shows dispersed aims, functional or spatial, to enhance the structural performance. (Nematzadeh & Fallah-Valukolae, 2021). Various studies have confirmed the existence of the shear span ratio on the shear capacity of concrete beams without stirrup. This section will briefly describe the five different empirical, analytical and artificial shear prediction models found in previous studies on ISF-reinforced concrete beams. According to a brief review, the limited proposed formula prescribes provisions that include the shear-enhancing effect of steel fibre combined with high-strength concrete. Song and Hwang [8] posit that the synergistic interaction among fibre, cement, and aggregates will undergo a change, implying that the equations currently utilized for normal-strength concrete will no longer be capable of predicting the mechanical properties of high-strength concrete. Table 5 demonstrates an overview of formulas focusing on describing the relationship between steel fibre with high-strength concrete in the current codes and guidelines, while Table 6 is built to compare the predicting ability of each formula.

Table 5

Review of proposed formula.

	Formula
Mansur et al.	$V_{frc} = (0.16\sqrt{f_{ck}} + 17.2\frac{\rho V_d}{M}) \leq 0.29\sqrt{f_{ck}}bd$
Al-Ta'an et al.	$v_{frc} = (1.6\sqrt{f_{ck}} + 960\rho_1\frac{d}{a}e + 8.5\rho V_f\frac{l_f}{d_f})/9$
Khuntia et al.	$v_{frc} = (0.167\alpha + 0.28V_f\frac{l_f}{d_f})\sqrt{f_{ck}}$
Swamy et al.	$v_{frc} = v_c + v_w = 3.75\tau_r + 0.9\sigma_{cu}$
Kara et al.	$v_{frc} = (\frac{\rho_1 d}{c_0 c_1 (\frac{a}{d})})^3 + \frac{F_1 d^4}{c_2} + \frac{c_3 \sqrt{f_{ck}}}{d^2}$
Ashour et al.	$v_{frc} = \left[(2.11\sqrt[3]{f_{ck}} + 7V_f\frac{l_f}{d_f})(\rho\frac{d}{a})^{0.333} \right]$ for $a/d \geq 2.5$ $v_{frc} = \left[(2.11\sqrt[3]{f_{ck}} + 7V_f\frac{l_f}{d_f})(\rho\frac{d}{a})^{0.333} \right] \left(\frac{2.5}{a} \right) + (0.41\tau_r V_f\frac{l_f}{d_f})(2.5 - \frac{d}{a})$ for $a/d < 2.5$

* V_{frc} is the shear capacity of fibre reinforced concrete beams; f_{ck} is the compressive strength of fibre reinforced concrete; ρ is the longitudinal ratio; b is the width of concrete beams; d is the depth of concrete beams; V_f is the fibre content and $\frac{l_f}{d_f}$ is the aspect ratio.

5.1.1. Prediction model of Mansur et al. (1986)

Due to the complexity of shear-related issues in concrete, there are proven to be challenging to resolve through purely analytical predictions. In that cases, a simplified model was introduced by Mansur, Ong and Paramasivam [13], which is based on a combination of rational analysis, test evidence, and successful structural performance experience. Mansur, Ong and Paramasivam [13] establish the model based on the ACI Committee 544. Moreover, there are four essential parameters considered in the prediction model:

- (1) The concrete compression zone, V_{cy}
- (2) aggregate interlock action, V_a
- (3) dowel action of longitudinal bars, V_d
- (4) web reinforcement by fibre, V_s

This analytical approach is primarily developed by considering the equilibrium of forces across a diagonal crack. Except the shear resist provided by fibre, the other parts can be lumped together and explained by V_c (The shear resist provided by concrete). In that case, the shear capacity of ISF reinforced concrete beams (V_{frc}) can be calculated by following formulas:

$$V_{frc} = V_{cy} + V_a + V_d + V_s \quad (1)$$

$$V_{frc} = V_c + V_s \quad \text{and} \quad V_c = V_{cy} + V_a + V_d \quad (2)$$

The V_{frc} calculated based on the ACI-ASCE Committee 426:

$$V_{frc} = \left(0.16\sqrt{f_{ck}} + 17.2\frac{\rho V_d}{M} \right) \leq 0.29\sqrt{f_{ck}}bd \quad (3)$$

The ρ is the longitudinal steel ratio, f_c is the concrete strength, b and d are the effective width and depth of the beams. The V/M is the ratio of external shear to moment at the section, and can be calculated by following formulas:

$$\frac{M}{V} = \frac{M_{max}}{V} - \frac{d}{2} \quad a \leq 2d \quad (4)$$

$$\frac{M}{V} = \frac{M_{max}}{V} - d \quad a > 2d \quad (5)$$

The shear resist provide by ISF are calculated by:

Table 6

Summary of Prediction Results versus Experimental Results.

Shear Span Ratio	1.5			2.5			3.5			4		
Fibre Content	0%	0.40%	0.80%	0%	0.40%	0.80%	0%	0.40%	0.80%	0%	0.40%	0.80%
Ratio between Prediction Results and Experimental Result for ISF reinforced beams												
Khuntia	0.59	1.87	1.91	0.81	0.41	0.92	0.62	0.69	0.40	0.42	0.72	0.69
Swamy	0.36	1.18	1.24	0.81	0.39	0.84	0.62	0.66	0.37	0.42	0.68	0.63
Mansur	0.47	1.50	1.53	0.86	0.42	0.91	0.64	0.69	0.39	0.43	0.71	0.66
Ashour	0.92	3.26	3.58	1.06	0.50	1.05	0.72	0.75	0.41	0.47	0.74	0.68
Ilker Fatih Kara	0.63	1.90	1.88	1.18	0.54	1.12	0.87	0.88	0.47	0.59	0.91	0.81
Al-Ta	0.84	2.34	2.17	1.53	0.64	1.23	0.96	0.91	0.46	0.62	0.90	0.76
Proposed Formulas in this Study	1.13	1.37	1.00	0.94	1.36	1.16	1.12	0.89	1.15	0.98	1.08	0.78
Ratio between Prediction Results and Experimental Result for RSF reinforced beams												
RSF Pre (MPa)	-	4.44	2.11	-	2.02	1.90	-	4.74	2.26	-	2.16	2.03
RSF Exp (MPa)	-	3.83	1.92	-	2.03	1.96	-	4.82	2.33	-	2.26	2.61
Pre/Exp	-	1.16	1.10	-	0.99	0.97	-	0.98	0.97	-	0.95	0.78

$$V_s = \sigma_{cu} b d \# \quad (6)$$

$$\sigma_{cu} = \eta_0 \eta_L \eta_b 2\tau \frac{l_f}{d_f} V_f \# \quad (7)$$

The σ_{cu} is the ultimate strength in tension of composite, and the formula of σ_{cu} provided by Swamy and Sa'ad [34]. The η_0 is orientation factor which is 0.41, and the η_b is the bond efficiency factor equals to 1 suggested by Swamy and Sa'ad [34]. l_f and d_f are the length and diameter of fibre, and V_f represents the volume of fibre. The fibre bond stress, τ was assumed to exist along $\frac{1}{4}$ of the fibre length and Visser and Boshoff [35] suggests the τ equal to $0.8\sqrt{f_c}$ for hooked ISF. The η_L is the length correction factor which can be calculated as:

$$\eta_L = 1 - \frac{\tan(\beta l_f / 2) h}{(\beta l_f / 2) \#} \quad (8)$$

$$\beta = \sqrt{\frac{2\pi G_m}{E_f A_f \ln\left(\frac{S}{r_f}\right)}} \quad (9)$$

$$S = 25 \sqrt{\frac{d_f}{V_f l_f}} \# \quad (10)$$

Where G_m is the matrix shear modules, A_f is the fibre cross-sectional area, r_f is the fibre radius and S is the mean centroid spacing. In this model, the contribution of concrete and fibre in shear capacity are described well, and the shear span ratio are considered in beginning. However, there are certain defects in the division of the shear span ratio, which result in a big gap between prediction and experiment value with the shear span ratio greater than 3.

5.1.2. Prediction Model of Al-Ta'an et al. (1990)

Al-Ta'an and Al-Feel [36] collected the test results of 89 ISF reinforced concrete beams, and focused on six parameters:

- (1) The compressive strength of concrete
- (2) Shear span ratio
- (3) Volume of fibres
- (4) Aspect ratio of fibre
- (5) Fiber types
- (6) Reinforcement ratio

The formula provided by Al-Ta'an and Al-Feel [36] based on the regression analysis with 89 experiment results. Besides the researchers highlighted the effect of interfacial bond stress and suggested an average value of 4.15 MPa can be used in the formula.

$$v_{fc} = \frac{1.6\sqrt{f_{ck}} + 960\rho_1 \frac{d}{a} e + 8.5\beta V_f \frac{l_f}{d_f}}{9} \# \quad (11)$$

Where e is the dimensionless factor, and can be calculated by following equation:

$$e = 1.0 \text{ when } a/d > 2.5$$

$$e = 2.5d/a \text{ when } a/d < 2.5$$

The expression based on the variables test beams and regression analysis which more accuracy than other formulas.

5.1.3. Prediction model of Khuntia, Stojadinovic and Goel [37]

Khuntia, Stojadinovic and Goel [37] introduced a straightforward analytical shear prediction model grounded on the ACI Committee 381. They suggested that the shear capacity of the ISF reinforced beam could be separated into two distinct components:

- (1) The shear strength provided by V_c
- (2) Shear strength provided by fibre: V_f

The V_c and V_f can be described simply by following equation:

$$v_c = 0.167\sqrt{f_{ck}} \# \quad (12)$$

$$v_f = A\beta\tau V_f \frac{l_f}{d_f} \# \quad (13)$$

Where A is the nondimensional constant which is 0.41 respectively. The β is the fibre factor which taken as 1 for hooked or crimped steel fibre suggested by Narayanan and Darwish (1992). The τ is the bond stress which equal to $0.68\sqrt{f_{ck}}$. In that case, the shear contribution of the fibres V_f becomes:

$$v_f = A\beta\tau V_f \frac{l_f}{d_f} = 0.41 \times 0.68 \times \sqrt{f_{ck}} \times V_f \frac{l_f}{d_f} = 0.28\sqrt{f_{ck}} V_f \frac{l_f}{d_f} \# \quad (14)$$

And the V_{fc} can be summary as:

$$v_{fc} = \left(0.167\alpha + 0.28V_f \frac{l_f}{d_f}\right) \sqrt{f_{ck}} \# \quad (15)$$

The author introduced the α as the arch action factor, which equal to $2.5d/a$. The formula provided by Khuntia, Stojadinovic and Goel [37] is a simplified equation which focus on both normal and high strength steel fibre reinforced beams. Besides, the prediction results have been validated conversation.

5.1.4. Prediction model of Swamy, Jones and Chiam [38]

Swamy, Jones and Chiam [38] described a simple analytical shear prediction model and focus on compression chord V_c and web

reinforcement V_w .

$$v_{frc} = v_c + v_w = 3.75\tau_r + 0.9\sigma_{cu}\# \quad (16)$$

Where σ_{cu} is the post-cracking tensile strength of fibre concrete, and the τ_r is the concrete shear strength which depend on the compressive strength. For the σ_{cu} , the author given following equation:

$$\sigma_{cu} = \eta_0 \eta_L \sigma_{fu} V_f \# \quad (17)$$

Where η_0 is orientation factor which is 0.41 suggested by author, and the η_L is the length efficiency factor of fibres equals to $0.98 \approx 1$ suggested by Laws, Lawrence and Nurse [39]. The σ_{fu} is the fibre fracture stress and V_f is the fibre content.

5.1.5. Prediction model of Kara (2013)

Kara [40] proposed a shear capacity prediction model based on gene expression programming. The fibre factor is determined by fibre type, volume of fibre and aspect ratio of fibre. With the help of 101 sets, the following formula can be drawn:

$$v_{frc} = \left(\frac{\rho_1 d}{c_0 c_1 \left(\frac{a}{d} \right)} \right)^3 + \frac{F_1 d^{\frac{1}{2}}}{c_2} + \frac{c_3^{\frac{1}{2}} \sqrt{f_{ck}}}{d^{\frac{1}{2}}} \# \quad (18)$$

$$F_1 = \beta V_f \frac{l_f}{d_f} \# \quad (19)$$

Where c_0 , c_1 , c_2 and c_3 are constants which equal to $c_0 = 3.324$, $c_1 = 0.909$, $c_2 = 2.289$ and $c_3 = 9.436$, respectively.

5.1.6. Prediction Model of Ashour, Hasanain and Wafa [41]

Ashour, Hasanain and Wafa [41] described a shear capacity formula based on the regression analysis. The author focuses on the shear capacity contribution provided by compressive strength of concrete and shear span ratio:

$$v_{frc} = \left(2.11 \sqrt[3]{f_{ck}} + 7V_f \frac{l_f}{d_f} \right) \left(\rho \frac{d}{a} \right)^{0.333} \# \quad (20)$$

This formula demonstrates robust predictive power for both normal and high-strength concrete beams tested by them. However, it undervalues the contribution of fibre, and the prediction outcomes for beams with low reinforcement ratios ($<0.37\%$) have some discrepancies when compared with experimental results.

According to the previous formula, it can be seen directly that there are several key parameters considered in the formula design: compressive strength, fibre content, longitudinal ratio, and fibre aspect ratio. Although the effect of the shear span ratio has been confirmed by many experiments, due to the different types of fibre, the explanations and equations about the shear capacity of fibre-reinforced concrete are distinct. In the present study, the influence of the shear-span ratio on the shear capacity of RSF and ISF reinforced beams are investigated by experiments. Furthermore, a novel theoretical formula for quantitatively describing the shear capacity of RSF reinforced concrete considering the shear-span ratio is proposed and verified.

According to the previous formula, several vital parameters should be considered in the formula design: compressive strength, fibre content, longitudinal ratio, and fibre aspect ratio. Although previous experiments have confirmed the effect of the shear span ratio, the explanations and equations about the shear capacity of fibre-reinforced concrete are distinct. Experiments in the present study has examined the influence of the shear-span ratio on the shear capacity of RSF and ISF-reinforced beams. Furthermore, a novel theoretical formula for quantitatively describing the shear capacity of RSF-reinforced concrete considering the shear-span ratio is proposed and verified.

5.2. Modify the TR63

Based on the analysis, Eourcode2 and TR63 are reasonably proposed as modifications to the current standard. In this study, several empirical equations are based on the Eurocode 2 and TR63, making it easier to predict the shear strength of the studied and collected beams. Moreover, 164 beams collected from published papers about the high-strength steel-fibre reinforced concrete beams have been evaluated to improve the predicting ability during regression analysis, with the details shown in Table Appendix A-2.

According to the proposed formula, five parameters are considered in the formula design: compressive strength (f_{ck}), longitudinal ratio (ρ), fibre content (V_f), shear span ratio ($\frac{d}{a}$), and fibre aspect ratio ($\frac{l_f}{d_f}$). Therefore, this section quantifies the beam model based on the following assumptions. Firstly, fibre-reinforced concrete beams are considered an ideal elastoplastic material under tension. Secondly, the shear force can be developed with plain reinforced concrete (RC) beams and fibre contributions. Thirdly, the fibre positions in the beams are random, assumably evenly distributed in the interior of the beam. The empirical equation for predicting the ultimate shear strength of the studied beams in this study is developed as follows: $V = V_c + V_f$.

5.2.1. RC beams

According to the design standard of TR63 and Eurocode 2, the shear capacity of RC beams should follow Eq. (21):

$$V_{Rd,c} = \left[C_{Rd,c} k (100 \rho f_{ck})^{\frac{1}{3}} \right] \quad (21)$$

However, the contribution of shear span ratios has not been individually proved. Based on the Eourcode2 and experimental results collected from published papers for the formula design, Eqs. (22 and 23) are built based on regression analysis:

$$V_{Rd,c} = 1.9 C_{Rd,c} k \sqrt[3]{100 \rho f_{ck} \frac{d}{a}} \quad \frac{a}{d} \leq 2.5 \quad (22)$$

$$V_{Rd,c} = \left[1.9 C_{Rd,c} k^{\frac{1}{3}} \sqrt[3]{100 \rho f_{ck} \frac{d}{a}} \right] \left(\frac{2.5}{\frac{a}{d}} \right) \quad \frac{a}{d} > 2.5 \quad (23)$$

where $C_{Rd,c}$ is the $0.18/\gamma_c$; k is constantly 0.15; f_c refers to the compressive strength in MPa, and a/d stands for the shear span ratio.

5.2.2. Fibre-reinforced Concrete Beams

According to TR63, the fibre contributions are based on the experiments of residual flexural strength. However, most collected results fail to include the residual flexural strength. To evaluate the residual flexural strength of fibre-reinforced concrete, the formula proposed by Venkateshwaran, Tan and Li [42] describes the contribution of the fibre effect in this study:

$$f_{R,4k} = \psi \left[0.177 (f_{ck})^{0.5} + 6.151 (RI) + 0.137 N^2 \right] \# \quad (24)$$

where $\psi = (1 + \frac{L_f}{100})^{0.5}$ and L_f are the fibre length; RI refers to the fibre factors, and ($V_f L_f / D_f$) and N stands for the number of hooked ends in steel fibre.

Based on the regression analysis and the evaluation of the impact of parameters, Formulas 21 to 28 have been determined for the shear capacity of the high-strength ISF and RSF-reinforced fibre beams. In addition, when considering the size effect, some beams with a shear span ratio less than 2.5 are collected, aiming to describe the shear capacity of the deep beams, while Table 6 has been made to describe the predicting ability between the proposed and previous formulas. In the formulas of Eqs. 25 to 28, this study considers the shear-span ratio as an important parameter and use regression analysis to adjust the coefficients based on

our experimental data. This statistical approach is essential for estimating relationships between variables, helping to accurately describe how different parameters affect the shear strength of ISF and RSF concrete beams. Through the regression process, large data sets from experiments to prediction results adjust coefficients in existing formulas to enhance the prediction ability. In the next section, this study will do a comprehensive evaluation to the proposed formula.

For the ISF reinforced concrete beams:

$$V_{Rd,c} = 1.15C_{Rd,c}k\sqrt{100\rho f_{ck}\frac{d}{a}} + 5\frac{f_{RA}}{\psi\sqrt{f_c}}\left(\rho\frac{d}{a}\right)^{\frac{1}{3}} \quad \frac{a}{d} > 2.5 \# \quad (25)$$

$$V_{Rd,c} = \left(\frac{2.5}{a}\right) * \left[C_{Rd,c}k\sqrt{100\rho f_{ck}\frac{d}{a}} + 5\frac{f_{RA}}{\psi\sqrt{f_c}}\left(\rho\frac{d}{a}\right)^{\frac{1}{3}} \right] \quad \frac{a}{d} \leq 2.5 \# \# \quad (26)$$

For the RSF reinforced concrete beams:

$$V_{Rd,c} = 1.15C_{Rd,c}k\sqrt{100\rho f_{ck}\frac{d}{a}} + 3\left(\rho\frac{d}{a}\right)^{\frac{1}{3}} \quad \frac{a}{d} > 2.5 \# \quad (27)$$

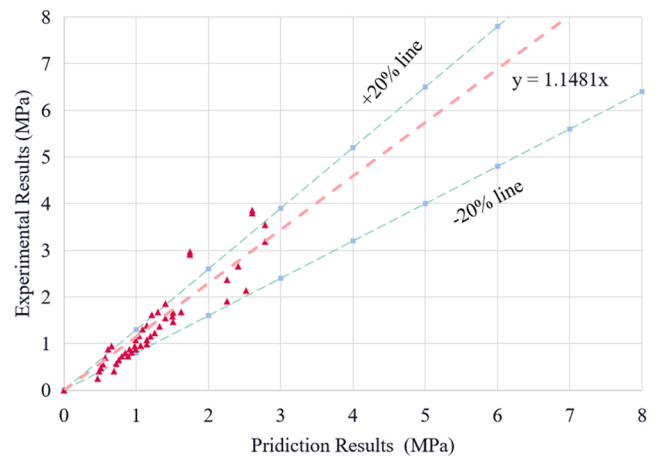
$$V_{Rd,c} = \left(\frac{2.5}{a}\right) * \left[C_{Rd,c}k\sqrt{100\rho f_{ck}\frac{d}{a}} + 3\frac{f_{RA}}{\psi\sqrt{f_c}}\left(\rho\frac{d}{a}\right)^{\frac{1}{3}} \right] \quad \frac{a}{d} \leq 2.5 \# \quad (28)$$

5.2.3. Evaluation of proposed model

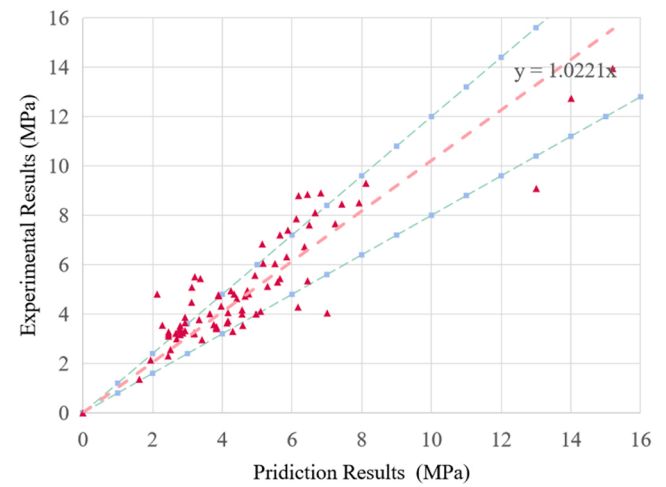
The proposed shear model undergoes evaluation by comparing its shear predictions to the experimental shear strengths obtained from 164 beam tests, which were conducted on a range of shear span ratios and included hooked-end ISF with fibre volumes from 0% to 4%. All these proposed formulas regarding the shear capacity of the high-strength concrete beam with steel fibre have been modified based on TR63 and Eurocode 2. Fig. 11 aims to indict the predicting ability of each formula, which is summarised in Table 6.

The statistical analysis shows that the average prediction-experimental value is 0.98 for the total dataset, with the standard deviation below 20% for most points, respectively. The model put forth in this study exhibits considerable effectiveness in predicting slightly conservative shear strengths, yielding a high accuracy χ of 0.95 and a low standard deviation (SD) of 0.10, which is desirable. Fig. 11 shows the calculated values of the shear strength with Eq. (15) versus the experimental values. The mean value of the calculated to the experimental was 0.965, 0.980, and 0.993, with a standard deviation of 0.222, 0.225 and 0.200 with RC, $a/d < 2.5$ datasets, and $a/d \geq 2.5$ datasets, respectively.

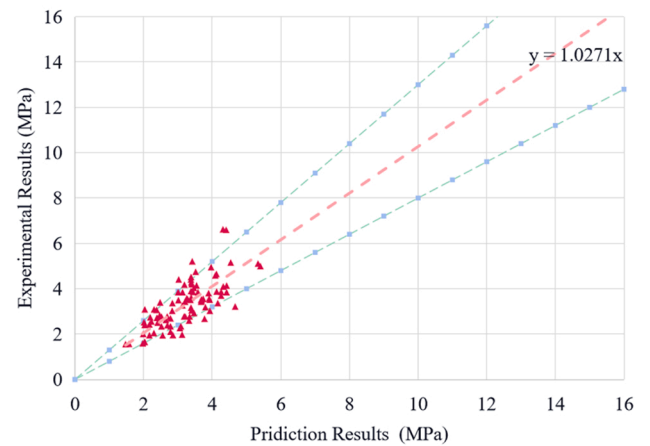
Moreover, to evaluate the f_{Exp}/f_{Pre} distributions in the datasets, box and whisker diagrams are drawn in Fig. 12, in which the calculated results are in an acceptable agreement with experimental values. This type of plot is based on a five-number summary: the minimum, first quartile, median, third quartile, and maximum. The "box" in the plot represents the interquartile range (IQR), which contains the middle 50% of the data. The "whiskers" extend to the smallest and largest values within 1.5 times the IQR from the first and third quartiles, respectively. Data points that fall outside of the whiskers are considered outliers, which are individually marked in the plot. This method of data representation is widely accepted in statistical analysis as it offers a straightforward way to identify potential outliers based on a mathematical definition. In the analysis, it should be paid attention to the position of outliers, most of which were observed to be in the upper region, indicating higher shear strengths in experiments. Due to the safe design principles and to foster more accurate predictions, this study adopted a strategy to underestimate the shear strength of beams deliberately. This approach is grounded in a cautious perspective that prefers to include data representing beams with lower shear values, thereby



(a) RC beams



(b) ISF reinforced concrete beams with shear span ratio higher than 2.5



(c) ISF reinforced concrete beams with shear span ratio lower than 2.5

Fig. 11. : Prediction Results versus Experimental Results.

ensuring safety in the design predictions. During extensive experimentation, the emergence of outliers is a common phenomenon. The methodology employed in this study, which utilizes a conservative approach for estimating shear force, exhibits a considerable degree of leniency towards outliers with lower experimental values. Consequently, this tolerance inadvertently leads to the categorization of certain data points as outliers, despite them not representing

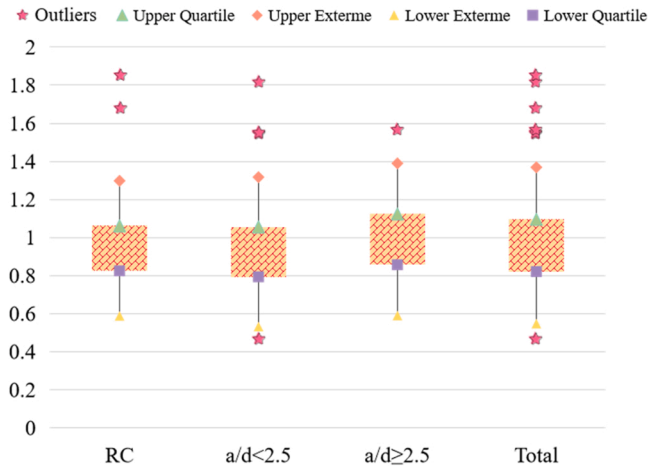


Fig. 12. : Box and whisker analysis for formula design.

exceptionally high experimental values.

Consequently, the series of formulas proposed in this study are designed to provide more accurate predictions compared to previous models, aligning closely with the principles of safe design. This methodology significantly limits the bias that might arise from giving undue weight to beams exhibiting ultra-high performance in shear resistance, thereby promoting safer design outcomes. Despite the conservative approach in handling the outliers, the proposed model effectively predicts the shear strength of ISF and RSF reinforced concrete beams across different shear span ratios, showcasing its reliability and robustness in shear strength prediction.

According to Table 6, the proposed formulas for RSF beams generally exhibit good predictive accuracy, with the ratio of predicted to experimental results ranging between 0.78 and 1.16. It is noteworthy that, despite a couple of predictions skewing towards the higher end of this range, the majority of the predicted values are closely aligned with the experimental results, towards a ratio of approximately 1 mostly. This demonstrates the high predictive capability of proposed model. However, due to a comprehensive database of test results for RSF reinforced beams was unavailable, this study can only re-structure formulas based on limited experiments results. It is recommend conducting more similar tests to accumulate a larger database, which would be instrumental in further validate the proposed model to achieve even higher predictive accuracy.

6. Sustainable development framework

6.1. Recycled steel fibre

The raw materials of RSF have been collected from the tyre-recycling company of Xiang He in Shanghai city, with the details of the manufacturing process shown in Fig. 13, which the price of the bead wires is 411€ per ton. Besides, the machine used to separate the bead wires is known as tyre spinning machine, with the details of the technical specifications shown in Table 7. The process of recycling is based on the following steps: 1) Waste tire collection; 2) Bead wires splitting; 3) Cleaning; 4) Shaping and application.

According to Table 7, the average tire can be dealt with is 40 piece per hour, with each hour consuming 16.5 kw/h. The weight of a recycled tire is around 9 kg [43]. Moreover, the percentage of the steel wires in a tire is 10–15% [44]. Therefore, Formula 29 can be used to calculate the GHG emissions of RSF:

$$Q_{RSF} = Q_e \rho_e * \theta * \gamma \quad (29)$$

where Q_{RSF} is the GHG emissions when recycling the waste bead wires from tires, whose unit is kg CO₂ eq; Q_e stands for the electricity



Fig. 13. : Manufacturing Process of RSF.

Table 7

Technical Specification of the tire spinning machine.

Name	Process Capacity (pc/h)	Equipment's power (kw)	Size of Tire (mm)
GRT	20–60	11–22	800–1200

consumed by the tire spinning machine whose unit is kw/h; ρ_e refers to the percentage of wires in the tires; θ presents the pieces of recyclable tires can be recycled per hours, whose unit is pc/h: and the γ demonstrates the GHG conversion factor.

6.2. GHG emissions of beams

To evaluate the possibility of replacing the ISF with RSF in sustainable construction development, the GHG emission and the material price of each beam are summarised in Table 8. Meanwhile, Table 9 illustrates the GHG emission values of beams obtained for the concrete mixes as shown in Table 1. Notably, the beams with different shear span ratios have a GWP between 1.85 and 5.04 kg CO₂ eq without any other fibre addition. Therefore, replacing ISF with RSF demonstrates reductions in GWP between 0.33 and 1.73 kg CO₂ eq. For replacing ISF with a shear

Table 8

GHG emissions and Budget price associated with various raw materials.

Component of Concrete	GWP/ kg CO ₂ eq	Price/ \$/kg	Resource
Basic Concrete Composition			
Ordinary Portland Cement	0.884	0.125	Anderson and Moncaster[45] Ouellet-Plamondon and Habert [46]
Coarse Aggregates	0.00429	0.0099	Ouellet-Plamondon and Habert [46]
Fine Aggregates, Sand	0.0024	0.0099	Ouellet-Plamondon and Habert [46]
Water	0.00015	0.0016	Ouellet-Plamondon and Habert [46]
Supplementary Materials			
Steel Fibre	2.2	1	Qin and Kaewunruen[18]
Steel Rebar	0.72	1.2	Özdemir, Günkaya, Özkan, Ersen, Bilgiç and Banar[47]
Raw Recycled Steel Fibre	0.07	0.4	Proposed by Author

Table 9

GHG emissions and Budget price of each beams.

GHG Emission of Each Beams/ kg CO ₂ eq				
Shear Span	1.50	2.50	3.50	4.00
Plain	1.89	3.15	4.41	5.04
0.4% ISF	2.23	3.71	5.19	5.93
0.8% ISF	2.56	4.27	5.98	6.83
0.4% RSF	1.90	3.17	4.43	5.07
0.8% RSF	1.91	3.19	4.46	5.10
GHG Emission Saving w.r.t 0.4% ISF beams	-14.61%			
GHG Emission Saving w.r.t 0.8% ISF beams	-25.39%			
Building Budgets of Each Beams/ \$				
Shear Span	1.50	2.50	3.50	4.00
Plain	0.35	0.58	0.81	0.93
0.4% ISF	0.50	0.83	1.17	1.34
0.8% ISF	0.65	1.09	1.52	1.74
0.4% RSF	0.41	0.68	0.95	1.09
0.8% RSF	0.47	0.78	1.10	1.25
Price Saving w.r.t 0.4% ISF beams	-18.30%			
Price Saving w.r.t 0.8% ISF beams	-28.04%			

span ratio of 4 with a reference concrete with relatively high strength, the decrease in GHG has been around 14.61% (M1-RSF-4 versus M1-ISF-4) and the building budget saving was around 18.30%. Yet, for reference concrete beams with relatively low strength, this GHG emission increase has been around 17.99% (M1-ISF-4 versus M0-4) and 0.5% (M1-RSF-4 versus M0-4). On the other hand, for replacing ISF with 0.8% RSF, the decrease of GHG emission is around 25.39% (M2-RSF-4 versus M2-ISF-4), with a building budget saving, respectively. Furthermore, a higher decrease in GHG emissions will occur when the replacement ratio for ISF by RSF is 100% compared with the case of 50% replacement. Furthermore, with the increase of the shear span ratio, the contribution of RSF in reducing GHG emission becomes more significance.

7. Future work

Based on the experiments results, the RSF recycled from waste tires could be able to replace the ISF incorporated into structural component for a serious of field applications have huge potential impact (e.g., pavement, airport, and high-rise bridge). In addition, the contribution of RFS in a circular economy should not be ignored. With the application of circle economy, the waste can be minimized, and materials are reused at the end of their life cycle, which lead to safer and more sustainable production and consumption patterns, reducing the risk of accidents and environmental disasters. While the competitive pricing and impressive performance of RSF indicate its potential for sustainable applications in reinforced concrete (RC) structures, several challenges still need be paid attention before it can be widely applied. Future research should be focus on the concerns:

- **Evaluation principles of RSF:** There is a pressing need to establish a comprehensive set of evaluation method that can standardize the performance of RSF. Given the variability in RSF quality due to differences in supplier and recycling processes, which make it challenging to ensure its reliability in engineering applications.
- **Micro-structure analysis:** As noted in this study, RSF is covered by rubber dust, the effects of which on the microstructure remain unknown. It is unclear whether the presence of rubber and graphite particles could affect the bond between RSF and the concrete matrix. Microscopic experiments are essential to explore the bond strength of RSF and to discern the influence of these particles on the bonding mechanism.
- **Fatigue damage:** Since RSF is recycled from waste tires, it already suffering fatigue stress. A deeper exploration into its fatigue characteristics through extensive experimental analysis and theoretical backing is necessary.

- **Durability:** The durability of RSF remains a significant concern which need more experiments to validate it. The potential for corrosion, from varied recycling and preservation methods, introduces an element of unpredictability in its performance. Future studies should focus on these issues, more research into aspects such as freeze-thaw cycles and corrosivity should be focused.

8. Conclusion

This study presents the results of three-point shear tests on ISF and RSF reinforced beams with different examined parameters, including shear span ratios and fibre properties. In addition, several empirical formulas proposed based on the experimental results and regression analysis. Moreover, environmental and economic impacts of using RSF and ISF, incorporating GHG emissions and budget analyses, supplemented by a sensitivity study on RSF manufacturing. The conclusions drawn are as follows:

Secondly, the failure mode of specimens shifts depending on the shear span ratio and the reinforcement type. Specimens with a smaller ratio exhibit shear-compression failure, which transitions to shear-tension failure upon reinforcement with ISF or RSF. Larger ratios lead to diagonal-tension failure, with added fibre enhancing midpoint displacement due to a bridging effect, albeit with diminishing returns at consistent fibre levels.

Initially, the compressive strength of fibre-reinforced concrete increases with the increased fibre content, with ISF concrete slightly outperforming RSF concrete. The strength difference remains minimal, peaking at a 3.05 MPa discrepancy at 0.8% fibre content.

Secondly, the failure mode of specimens depend on the shear span ratio and the fibre content. Specimens with a smaller ratio exhibit shear-compression failure, which transitions to shear-tension failure upon reinforcement with ISF or RSF. Larger ratios lead to diagonal-tension failure, with added fibre enhancing midpoint displacement due to a bridging effect. However, the contribution gaps of the displacement increment with different types of steel fibre have become negligible in specimens when maintaining the same fibre.

Thirdly, compared to the beam specimens without fibre reinforcement, the steel fibre has reinforced concrete beam specimens with considerable larger load-carrying capacity and deformation. The presence of shear studs, such as the bridging effect, have dramatically enhanced the load-carrying capacity of both ISF and RSF-reinforced concrete specimens.

Furthermore, as a reference for the global warming potential (GWP) impact category, carbon emissions has been between 2.23 and 6.83 kg CO₂ eq for the high-strength fibre-reinforced concrete materials incorporating ISF. These values can be reduced by up to 14.61% by replacing 0.4% with RSF. In addition, 25.39% is obtained by replacing the 0.8% RSF. In addition, reducing budget price has been proved when replacing the RSF with ISF. When transportation distances have not been considered, the price budget can be reduced by up to 28.04% in than the 0.8% fibre content.

CRediT authorship contribution statement

Huang Xu: Writing – original draft, Visualization, Validation, Methodology, Investigation, Formal analysis, Data curation, Conceptualization. **Li Yang:** Writing – original draft, Validation, Investigation, Formal analysis, Data curation, Conceptualization. **Kaewunruen Sakdirat:** Writing – review & editing, Supervision, Resources, Project administration, Methodology, Investigation, Funding acquisition, Formal analysis, Data curation, Conceptualization. **Qin Xia:** Writing – review & editing, Writing – original draft, Visualization, Validation, Software, Methodology, Investigation, Formal analysis, Data curation, Conceptualization.

Declaration of Competing Interest

The authors declare that they have no known competing financial interests or personal relationships that could have appeared to influence the work reported in this paper.

Data Availability

Data will be made available on request.

Acknowledgments

The authors are grateful to the European Commission for the financial sponsorship of the H2020-RISE Project No. 691135 “RISEN: Rail Infrastructure Systems Engineering Network,” which enables a global research network that tackles the grand challenge in railway

infrastructure resilience and advanced sensing in extreme environments (www.risen2rail.eu) [47]. In addition, this project was partially supported by the European Commission’s Shift2Rail, H2020-S2R Project No. 730849 “S-Code: Switch and Crossing Optimal Design and Evaluation.” This article is partially based upon work from COST Action (Circular B — Implementation of Circular Economy in the Built Environment, CA21103), supported by COST (European Cooperation in Science and Technology). The APC has been kindly sponsored by the University of Birmingham Library’s Open Access Fund.

Author contributions

S.K developed the concept; X.Q did the data collection, and data analyzed; X.Q contributed the manuscript; S.K and X.Q reviewed the paper. All authors wrote the paper. All authors have read and agree to the published version of the manuscript.

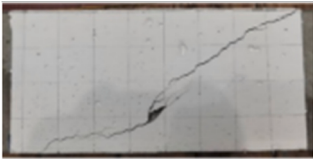
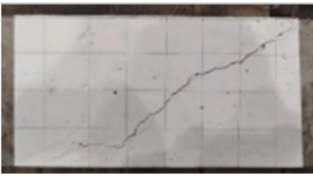
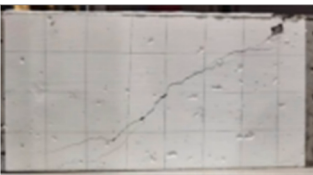

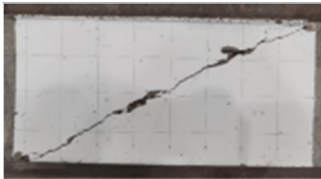
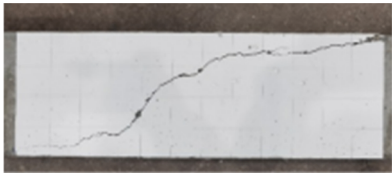

Appendix A

Table A1
Failure Mode of Beams.

Image	Beam information	Failure Mode
	M0-1.5 Max Load: 86.65 kN Max Displacement: 6.21 mm	Splitting Shear Failure
	M1-ISF-1.5 Max Load: 100.8 kN Max Displacement: 7.41 mm	Shear Compression Failure
	M2-ISF-1.5 Max Load: 129.92 kN Max Displacement: 7.89 mm	Shear Compression Failure
	M1-RSF-1.5 Max Load: 93.94 kN Max Displacement: 7.17 mm	Shear Compression Failure
	M2-RSF-1.5 Max Load: 118.07 kN Max Displacement: 8.10 mm	Shear Compression Failure

(continued on next page)

Table A1 (continued)

	M0-2.5 Max Load: 45.86 kN Max Displacement: 3.41 mm	Diagonal Tension Failure
	M1-ISF-2.5 Max Load: 77.67 kN Max Displacement: 5.59 mm	Diagonal Tension Failure
	M2-ISF-2.5 Max Load: 101.09 kN Max Displacement: 5.87 mm	Diagonal Tension Failure
	M1-RSF-2.5 Max Load: 64.60 kN Max Displacement: 3.84 mm	Diagonal Tension Failure
	M2-RSF-2.5 Max Load: 78.42 kN Max Displacement: 5.59 mm	Diagonal Tension Failure
	M0-3.5 Max Load: 84.58 kN Max Displacement: 5.16 mm	Diagonal Tension Failure
	M1-ISF-3.5 Max Load: 110.28 kN Max Displacement: 6.86 mm	Diagonal Tension Failure

(continued on next page)

Table A1 (continued)

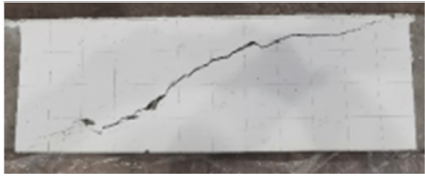
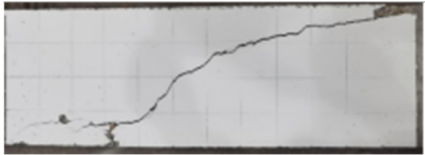

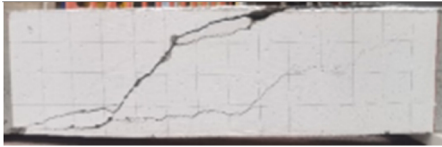
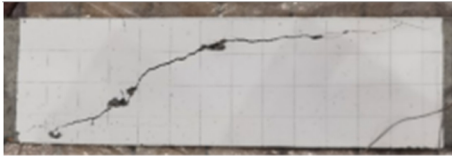

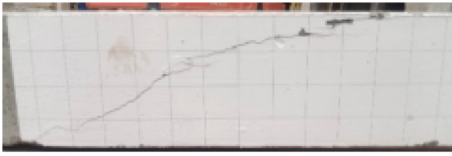
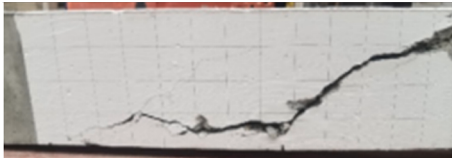
	M2-ISF-3.5 Max Load: 126.16 kN Max Displacement: 7.60 mm	Diagonal Tension Failure
	M1-RSF-3.5 Max Load: 109.49 kN Max Displacement: 5.44 mm	Diagonal Tension Failure
	M2-RSF-3.5 Max Load: 121.67 kN Max Displacement: 6.85 mm	Diagonal Tension Failure
	M0-4 Max Load: 119.78 kN Max Displacement: 7.94 mm	Diagonal Tension Failure
	M1-ISF-4 Max Load: 186.51 kN Max Displacement: 8.09 mm	Diagonal Tension Failure
	M2-ISF-4 Max Load: 235.42 kN Max Displacement: 9.05 mm	Diagonal Tension Failure
	M1-RSF-4 Max Load: 150.74 kN Max Displacement: 9.67 mm	Diagonal Tension Failure
	M2-RSF-4 Max Load: 200.09 kN Max Displacement: 9.61 mm	Diagonal Tension Failure

Table A2
Datasets.

Author	Number of Beam	Compressive Strength MPa	Fibre Content %	Longitudinal Ratio %	Shear Span	Cross Section (W*D) mm	Fibre Type
Ashour, Hasanain and Wafa [41]	18	92 ~101.32	0.5–1.5	0.37–4.58	1, 2, 4, 6	125 * 215	Hooked
Yoo and Yang [48]	3	62.3	0.75	1.5	2, 4, 6	300 * 420 450 * 648 600 * 887	Hooked
Manju, Sathya and Sylviya [49]	6	82–83.8	0.5–1.5	1	1.5, 2.5	185 * 220	Hooked
Tahenni, Chemrouk and Lecompte [50]	16	63.1–65	0–3	1.16–1.5	2.2	100 * 135	Hooked
Kwak, Eberhard, Kim and Kim [51]	9	62.6–68.6	0–0.75	1.5	2, 3, 4	125 * 212	Hooked
Alzahrani [52]	6	61.6–73	0–0.75	1.46	3	200 * 350	Hooked
Singh and Jain [53]	9	53.4–64.6	0.75–1.5	2.67	3.49	150 * 253	Hooked
Vandewalle and Mortelmans [12]	16	108.5–112	0–0.75	1.87	1.75, 2.5, 3.5, 4.5	200 * 300	Hooked
Cho and Kim [54]	14	54.3–89.9	0–2	1.3–2.9	1.05	120 * 167.5	Hooked
Narayanan and Darwish [55]	20	57.3–65.8	0.25–3	2–5.72	2, 2.5, 3	130 * 130	Crimped
Shin, Oh and Gosh [56]	13	80	0–1	3.59	2, 3, 4.5, 6	100 * 175	Plain
Noghabai [57]	17	72–93.3	0.5–1	2.87–4.47	2.77–3.33	200 * 180 200 * 235 200 * 410 300 * 570	Plain and Hooked
Uomoto, Weerarathe, Furukoshi and Fujino [58]	4	54	1.5	2.2	1.5–2.5	182 * 182	Plain
Hwang, Lee, Kim, Ju and Seo [59]	3	58–88	0.5–1	4.78	3	100 * 165	Hooked
Li, Ward and Hamza [60]	10	62.6	1	1.1–3.3	1–3	63.5 * 102	Crimped

References

- [1] Y.K. Peng, The effect of carbon black and silica fillers on cure characteristics and mechanical properties of breaker compounds, Master of Science Thesis (2007).
- [2] J. Mei, G. Xu, W. Ahmad, K. Khan, M.N. Amin, F. Aslam, A. Alaskar, Promoting sustainable materials using recycled rubber in concrete: a review, *J. Clean. Prod.* (2022), 133927.
- [3] M. Sienkiewicz, J. Kucinska-Lipka, H. Janik, A. Balas, Progress in used tyres management in the European Union: a review, *Waste Manag.* 32 (10) (2012) 1742–1751.
- [4] P.T. Williams, Waste treatment and disposal, John Wiley & Sons., 2005.
- [5] H.R. Karimi, M. Aliha, P. Ebneabbasi, S. Salehi, E. Khedri, P.J. Haghighatpour, Mode I and mode II fracture toughness and fracture energy of cement concrete containing different percentages of coarse and fine recycled tire rubber granules, *Theor. Appl. Fract. Mech.* 123 (2023), 103722.
- [6] Y. Li, H. Li, G. Zhang, S. Kaewunruen, Nonlinear responses of longitudinally coupled slab tracks exposed to extreme heat waves, *Eng. Struct.* 281 (2023), 115789.
- [7] X. Liu, G.E. Thermou, A review on the shear performance of reinforced concrete (RC) beams strengthened with externally bonded mortar-based composites, *Structures*, Elsevier., 2023, 105474.
- [8] P. Song, S. Hwang, Mechanical properties of high-strength steel fiber-reinforced concrete, *Constr. Build. Mater.* 18 (9) (2004) 669–673.
- [9] H. Behbahani, B. Nematollahi, M. Farasatpour, Steel fiber reinforced concrete: a review, (2011).
- [10] E.O. Lantsoght, How do steel fibers improve the shear capacity of reinforced concrete beams without stirrups? Compos. Part B: Eng. 175 (2019), 107079.
- [11] S.H. Ahmad, A. Khaloo, A. Poveda, Shear capacity of reinforced high-strength concrete beams, *J. Proc.* (1986) 297–305.
- [12] M.I. Vandewalle, F. Mortelmans, Shear capacity of steel fiber high-strength concrete beams, *Spec. Publ.* 149 (1994) 227–242.
- [13] M. Mansur, K. Ong, P. Paramasivam, Shear strength of fibrous concrete beams without stirrups, *J. Struct. Eng.* 112 (9) (1986) 2066–2079.
- [14] S. Al-Ta'an, J. Al-Feel, Evaluation of shear strength of fibre-reinforced concrete beams, *Cem. Concr. Compos.* 12 (2) (1990) 87–94.
- [15] R. YB, N. Hossiney, D. HT, Properties of high strength concrete with reduced amount of Portland cement—a case study, *Cogent Eng.* 8 (1) (2021), 1938369.
- [16] Z. Zamanzadeh, L. Lourenço, J. Barros, Recycled steel fibre reinforced concrete failing in bending and in shear, *Constr. Build. Mater.* 85 (2015) 195–207.
- [17] F. Soltanzadeh, A.E. Behbahani, K. Hosseinmostofi, C.A. Teixeira, Assessment of the sustainability of fibre-reinforced concrete by considering both environmental and mechanical properties, *Sustainability* 14 (10) (2022) 6347.
- [18] X. Qin, S. Kaewunruen, Environment-friendly recycled steel fibre reinforced concrete, *Constr. Build. Mater.* 327 (2022), 126967.
- [19] P. Zhang, C. Wang, C. Wu, Y. Guo, Y. Li, J. Guo, A review on the properties of concrete reinforced with recycled steel fiber from waste tires, *Rev. Adv. Mater. Sci.* 61 (1) (2022) 276–291.
- [20] Y. Li, R.-H. Zhao, D.-Y. Li, C. Qu, Study on seismic performance of recycled steel fibers locally reinforced cruciform concrete frame beam-column joint, *Adv. Civ. Eng.* 2022 (2022).
- [21] B. Ali, R. Kurda, H. Ahmed, R. Alyousef, Effect of recycled tyre steel fiber on flexural toughness, residual strength, and chloride permeability of high-performance concrete (HPC), *J. Sustain. Cem. -Based Mater.* (2022) 1–17.
- [22] A. Abdul Awal, M.A.A. Kadir, L.L. Yee, N. Memon, Strength and deformation behaviour of concrete incorporating steel fibre from recycled tyre. CIEC 2014, Springer, 2015, pp. 109–117.
- [23] B.J. Dorr, C.L. Kanali, R.O. Onchiri, Shear Performance of Recycled Tyres Steel Fibres Reinforced Lightweight Concrete Beam using Palm Kernel Shear as Partial Replacement of Coarse Aggregate.
- [24] F. Grzymalski, M. Musiał, T. Trapko, Mechanical properties of fibre reinforced concrete with recycled fibres, *Constr. Build. Mater.* 198 (2019) 323–331.
- [25] F. Althoe, O. Zaid, F. Alsharari, A. Yosri, H.F. Islem, Evaluating the impact of nano-silica on characteristics of self-compacting geopolymer concrete with waste tire steel fiber, *Arch. Civ. Mech. Eng.* 23 (1) (2023) 1–17.
- [26] M. Polyakova, A. Stolyarov, Automobile Tires' High-Carbon Steel Wire, *Encyclopedia* 1 (3) (2021) 859–870.
- [27] X. Luo, W. Sun, S.Y.N. Chan, Effect of heating and cooling regimes on residual strength and microstructure of normal strength and high-performance concrete, *Cem. Concr. Res.* 30 (3) (2000) 379–383.
- [28] A.C. 363, ACI PRC-363.2–11 Guide to Quality Control and Assurance of High-Strength Concrete, (2011) 19.
- [29] L. Hussein, L. Amleh, Structural behavior of ultra-high performance fiber reinforced concrete-normal strength concrete or high strength concrete composite members, *Constr. Build. Mater.* 93 (2015) 1105–1116.
- [30] A.A. Shah, Y. Ribakov, Recent trends in steel fibered high-strength concrete, *Mater. Des.* 32 (8–9) (2011) 4122–4151.
- [31] H. Pam, A. Kwan, M. Islam, Flexural strength and ductility of reinforced normal- and high-strength concrete beams, *Proc. Inst. Civ. Eng. -Struct. Build.* 146 (4) (2001) 381–389.
- [32] B. Group, BS EN 197–1:2011 Cement Composition, specifications and conformity criteria for common cements, 2019–02-19, p. 56.
- [33] C. Johnston, Å. Skarendahl, Comparative flexural performance evaluation of steel fibre-reinforced concretes according to ASTM C1018 shows importance of fibre parameters, *Mater. Struct.* 25 (1992) 191–200.
- [34] R. Swamy, A. Sa'ad, Deformation and ultimate strength in flexure of reinforced concrete beams made with steel fiber concrete, *J. Proc.* (1981) 395–405.
- [35] D. Visser, W. Boshoff, Shear behaviour of concrete V-shaped beams with and without steel fibres, *J. Mater. Struct.* 54 (1) (2021) 1–23.
- [36] S. Al-Ta'an, J. Al-Feel, Evaluation of shear strength of fibre-reinforced concrete beams, *Cem. Concr. Compos.* 12 (2) (1990) 87–94.
- [37] M. Khuntia, B. Stojadinovic, S.C. Goel, Shear strength of normal and high-strength fiber reinforced concrete beams without stirrups, *Structural Journal* 95 (2) (1999) 282–289.
- [38] R.N. Swamy, R. Jones, A.T. Chiam, Influence of steel fibers on the shear resistance of lightweight concrete I-beams, *Struct. J.* 90 (1) (1993) 103–114.
- [39] V. Laws, P. Lawrence, R. Nurse, Reinforcement of brittle matrices by glass fibres, *J. Phys. D: Appl. Phys.* 6 (5) (1973) 523.
- [40] I.F. Kara, Empirical modeling of shear strength of steel fiber reinforced concrete beams by gene expression programming, *Neural Comput. Appl.* 23 (3) (2013) 823–834.

- [41] S.A. Ashour, G.S. Hasanain, F.F. Wafa, Shear behavior of high-strength fiber reinforced concrete beams, *Struct. J.* 89 (2) (1992) 176–184.
- [42] A. Venkateshwaran, K.H. Tan, Y. Li, Residual flexural strengths of steel fiber reinforced concrete with multiple hooked-end fibers, *Struct. Concr.* 19 (2) (2018) 352–365.
- [43] M. Balaha, A. Badawy, M. Hashish, Effect of using ground waste tire rubber as fine aggregate on the behaviour of concrete mixes, (2007).
- [44] L. Bockstal, T. Berchem, Q. Schmetz, A. Richel, Devulcanisation and reclaiming of tires and rubber by physical and chemical processes: A review, *J. Clean. Prod.* 236 (2019), 117574.
- [45] J. Anderson, A. Moncaster, Embodied carbon of concrete in buildings, part 1: analysis of published EPD, *Build. Cities* 1 (1) (2020).
- [46] C. Ouellet-Plamondon, G. Habert, Life cycle assessment (LCA) of alkali-activated cements and concretes, *Handbook of alkali-activated cements, mortars and concretes*, Elsevier, 2015, pp. 663–686.
- [47] A. Özdemir, Z. Günkaya, A. Özkan, O. Ersen, M. Bilgiç, M. Banar, Lifecycle assessment of steel rebar production with induction melting furnace: Case study in Turkey, *J. Hazard., Toxic., Radioact. Waste* 22 (2) (2018), 04017027.
- [48] D.-Y. Yoo, J.-M. Yang, Effects of stirrup, steel fiber, and beam size on shear behavior of high-strength concrete beams, *Cem. Concr. Compos.* 87 (2018) 137–148.
- [49] R. Manju, S. Sathya, B. Sylviya, Shear strength of high-strength steel fibre reinforced concrete rectangular beams, *Int J. Civ. Eng. Technol.* 8 (8) (2017) 1716–1729.
- [50] T. Tahenni, M. Chemrouk, T. Lecompte, Effect of steel fibers on the shear behavior of high strength concrete beams, *Constr. Build. Mater.* 105 (2016) 14–28.
- [51] Y.-K. Kwak, M.O. Eberhard, W.-S. Kim, J. Kim, Shear strength of steel fiber-reinforced concrete beams without stirrups, *Acids Struct. J.* 99 (4) (2002) 530–538.
- [52] F. Alzahrani, Shear behaviour of steel fibre-reinforced high strength lightweight concrete beams without web reinforcement, Memorial University of Newfoundland, 2018.
- [53] B. Singh, K. Jain, Appraisal of steel fibers as minimum shear reinforcement in concrete beams, *Acids Struct. J.* 111 (5) (2014).
- [54] S.-H. Cho, Y.-I. Kim, Effects of steel fibers on short beams loaded in shear, *Struct. J.* 100 (6) (2003) 765–774.
- [55] R. Narayanan, I. Darwish, Shear in mortar beams containing fibers and fly ash, *J. Struct. Eng.* 114 (1) (1988) 84–102.
- [56] S.-W. Shin, J.-G. Oh, S. Ghosh, Shear behavior of laboratory-sized high-strength concrete beams reinforced with bars and steel fibers, *Spec. Publ.* 142 (1994) 181–200.
- [57] K. Noghabai, Beams of fibrous concrete in shear and bending: experiment and model, *J. Struct. Eng.* 126 (2) (2000) 243–251.
- [58] T. Uomoto, R. Weeraratne, H. Furukoshi, H. Fujino, Shear strength of reinforced concrete beams with fiber reinforcement, *Proc. RILEM Symp. FRC*, 1986, pp. 553–562.
- [59] J.-H. Hwang, D.H. Lee, K.S. Kim, H. Ju, S.-Y. Seo, Evaluation of shear performance of steel fibre reinforced concrete beams using a modified smeared-truss model, *Mag. Concr. Res.* 65 (5) (2013) 283–296.
- [60] V.C. Li, R.J. Ward, A.M. Hamza, Steel and synthetic fibers as shear reinforcement, (1992).